NASA TECHNICAL NOTE

NASA TN D-5257

c. 1

NASA TN D-5257

A STUDY OF THE PERFORMANCE OF LOW-DENSITY PHENOLIC-NYLON ABLATORS

by James N. Moss and William E. Howell

Langley Research Center
Langley Station, Hampton, Va.

NATIONAL AERONAUTICS AND SPACE ADMINISTRATION • WASHINGTON, D. C. • JUNE 1969

A STUDY OF THE PERFORMANCE OF LOW-DENSITY PHENOLIC-NYLON ABLATORS

By James N. Moss and William E. Howell

Langley Research Center
Langley Station, Hampton, Va.

NATIONAL AERONAUTICS AND SPACE ADMINISTRATION

For sale by the Clearinghouse for Federal Scientific and Technical Information
Springfield, Virginia 22151 – CFSTI price $3.00

A STUDY OF THE PERFORMANCE OF LOW-DENSITY PHENOLIC-NYLON ABLATORS*

By James N. Moss and William E. Howell
Langley Research Center

SUMMARY

The performance of low-density (160 to 320 kg/m^3) phenolic-nylon ablative materials was evaluated experimentally. The ablative effectiveness of some of the low-density materials was about 1.5 times that of a 580 kg/m^3 phenolic-nylon ablator. Furthermore, it was found that a 220 kg/m^3 ablator provided high ablative effectiveness while maintaining good structural char integrity when exposed to a range of test conditions that included most environmental conditions experienced by a manned lifting-body entry vehicle.

In addition, an analysis was made of the mass requirements for an ablative heat shield of a blunted half-cone entry vehicle (one-half of a 13^o half-angle cone). The analysis shows that the mass of ablative heat shield required is strongly dependent on the entry attitude, decreasing with increasing angle of attack. A 34-percent reduction in the total mass of the ablative heat shield may be obtained by using a phenolic-nylon ablator with a density of 220 kg/m^3 rather than one with a density of 580 kg/m^3.

INTRODUCTION

Several studies have been made concerning the heat-shield mass requirements for lifting-body entry vehicles to be used for manned near-earth logistic-ferry applications. Some of the studies (refs. 1 and 2) have indicated that the heat-shield mass for lifting vehicles may range from 20 to 30 percent of the vehicle gross mass.

Of the basic heat-shield concepts available, the ablative heat shields are generally recommended (refs. 1 to 4) because of their high efficiency for the environment experienced by manned lifting-body entry vehicles. This environment is typified by relatively

---

*The basic information presented herein was included in a thesis entitled "A Study of the Potential Benefits of Using Lower-Density Ablators for Protecting Manned Lifting-Body Entry Vehicles," by James N. Moss, submitted in partial fulfillment of the requirements for the degree Master of Aerospace Engineering, University of Virginia, Charlottesville, Virginia, June 1968.

low heating rates and high total heat loads. This heating is predominantly convective since radiative heating is negligible for entry from near-earth orbits. Studies of some of the ablation materials available (ref. 5) have shown that the low-density char-forming ablators provide the most effective protection for this type of environment.

The use of charring ablators having densities less than 580 to 640 kg/m^3, that is, densities less than that for which most of the heat-shield design studies have been made, may be desirable if the lower density ablators can perform reliably. Consequently, the present investigation was undertaken to evaluate the performance of low-density (160 to 320 kg/m^3) phenolic-nylon ablative materials when subjected to test environments representative of that experienced by manned lifting-body entry vehicles and to determine by analysis the potential mass savings that may be realized by using a 220 kg/m^3 ablator rather than a 580 kg/m^3 ablator for a lifting-body entry vehicle at various entry attitudes. The analysis includes the determination of the trajectory parameters and the aerodynamic and heating characteristics of the vehicle (one-half of a 13^o half-angle cone with a spherically blunt tip) at the various entry attitudes.

SYMBOLS

The units used for the physical quantities defined in this paper are given in the International System of Units (SI). Factors relating the International System with other systems of units are given in reference 6.

C	oxygen concentration by mass, percent
C_L	lift coefficient
E	ablative effectiveness, defined as qt/m where t is the time for a back-surface temperature rise of 167^o K, joules/kilogram (J/kg)
H	total enthalpy, joules/kilogram (J/kg)
h	altitude, meters (m)
l	length of vehicle, meters (m)
L/D	lift-drag ratio
M	total mass of ablation material, kilograms (kg)

m	mass per unit area of uncharred ablation material, kilograms/meter^2 (kg/m^2)
p_t	stagnation pressure behind normal shock, atm (1 atm = 101.325 kN/m^2)
q	convective heating rate to a cold wall with no mass transfer, watts/meter^2 (W/m^2)
r	sphere radius, meters (m)
s	distance along a meridian on the surface of the lifting-body entry vehicle measured from geometric stagnation point, meters (m)
t	time, sec
V	velocity, meters/second (m/sec)
α	angle of attack, deg
γ	flight-path angle from horizontal, deg
ρ	density, kilograms/meter^3 (kg/m^3)
ϕ	roll angle, measured from the most windward streamline, deg

Subscripts:

e	edge of boundary layer
max	maximum
o	initial value
s	stagnation point
w	wall
1,2	different environments

TEST MODELS AND FACILITIES

Ablation Models

The phenolic-nylon ablation models considered in this study consisted of various percentages of powdered phenolic bonding material, nylon powders, and phenolic Microballoons as listed in tables I and II. Details regarding the material processing and fabrication of these materials are available in reference 7.

The test models were made by machining the fabricated phenolic-nylon composites into 7.6-cm disks with a thickness of 0.97 cm. The instrumentation and model configuration are shown in figure 1. A 0.95-cm-diameter 0.79-mm-thick copper heat sink, which had a thermocouple silver-soldered to its back surface, was affixed to the back surface of the ablation material. A mounting block was bonded to the back surface of the ablation models with a room-temperature vulcanizing rubber. The mounting block afforded a means of attachment to the specimen inserter and isolated the heat sink from the test environment.

Test Apparatus

The ablation models were tested in two supersonic arc tunnels at the Langley Research Center. The models listed in table I and some of the models in table II were tested in Apparatus B of the Langley entry structures facility; the remaining models in table II were tested in Apparatus D of the Langley entry structures facility.

Apparatus B.- A schematic diagram of Apparatus B is shown in figure 2. The range of operational parameters for this apparatus when equipped with a 9.65° conical nozzle with a 3.8-cm-diameter throat and a 15.2-cm-diameter exit, as used in this study, are included in table III. The arc facility utilizes a three-phase ac powered arc system to heat the test gas. The only limitation with respect to operating time for this facility is the vacuum capability, that is, the ability to maintain the desired pressure in the test section.

Apparatus D.- Apparatus D has essentially the same test section as Apparatus B but has a vortex-stabilized constricted dc arc heater and a diffuser that is connected to a steam ejector rather than to a vacuum sphere. The operational parameters for this facility when equipped with an 8.18° conical nozzle with a 2.5-cm-diameter throat and a 10.2-cm-diameter exit, as used in this study, are included in table III.

TEST CONDITIONS AND PROCEDURES

Test Conditions

The nominal test conditions for the ablation models of varying compositions and density are listed in table I. The ablation models of constant composition and density

that were subjected to various test conditions are listed in table II along with their respective test conditions.

Test Procedure

Prior to the test of the ablation models, the desired test condition was determined and calibrated with respect to heating rate and pressure. The procedure for each model tested was to start the facility and allow enough time for the test condition to become stable. A heating-rate measurement, obtained by the transient calorimetry technique, was taken and the test model was inserted with the model surface normal to the flow. The model exposure time was such that the copper heat sink on the back surface of the model would experience a temperature rise of 167° K. During the model exposure, the output from the thermocouple attached to the copper heat sink and the test-facility temperature and pressure data were recorded at 2-second intervals on digital tape. A second heating rate was obtained as soon as the test model was retracted from the test stream to obtain an average heating rate. The charred models were then cross-sectioned, photographed, and measured to determine surface recession.

EXPERIMENTAL RESULTS AND DISCUSSION

The objective of the experimental program was to determine whether low-density $(160$ to 320 kg/m$^3)$ phenolic-nylon ablation materials that could be fabricated would perform satisfactorily when exposed to simulated entry environments obtainable in supersonic arc test facilities. The performance of a number of low-density phenolic-nylon ablators having different densities and compositions was determined experimentally for the test conditions given in table I. Once this phase of the experimental study was completed, one ablator was selected for a more extensive evaluation by exposing it to a number of test environments. The results of the arc-tunnel tests of phenolic-nylon materials are listed in tables I and II and are discussed in detail subsequently.

Extent to Which Test Conditions Simulated Entry Environment

Since it is not possible, in general, to provide a complete simulation of entry conditions in ground test facilities for ablation studies, the approach has been to determine the more important environmental parameters involved in the ablation process and to concentrate on scaling the test environment so that these parameters are simulated. The following relation

$$\frac{(C_e - C_w)_1}{(C_e - C_w)_2} = \frac{(H_e - H_w)_1}{(H_e - H_w)_2}$$

which is presented in reference 8, was the basis for reducing the test-stream oxygen concentration from that of air for the tests conducted in the relatively low-enthalpy environment produced in Apparatus B. A comparison of the experimental test conditions (table III) with typical lifting-body entry conditions (figs. 14 and 15) indicates that a good simulation of the entry conditions experienced by a manned lifting-body entry vehicle was obtained at several times during the entry trajectory. This observation is based on the assumption that the net convective heating (ref. 8), the total stream enthalpy H_e and the stream oxygen concentration C_e are the important environmental parameters which determine the ablative performance of phenolic-nylon ablators subjected to environments experienced by manned lifting-body entry vehicles.

Performance of Various Materials

The phenolic-nylon materials listed in table I, as well as those in table II, were compared on the basis of the ablative effectiveness E and the physical appearance of the charred material. The ablative effectiveness is defined as follows:

$$E = \frac{qt}{m}$$

where q is the cold-wall heating rate to a nonablating surface, t is the time for a back-surface temperature rise of 167° K, and m is the initial mass per unit area of uncharred ablation material used. The back-surface temperature rise of 167° K, even though arbitrary, has often been used in previous studies, for example, references 5, 7, and 8. Consequently, the effectiveness values listed in this report can be compared with previous results. The value of the effectiveness parameter depends on both the mass loss characteristics and the insulating properties of materials. Although the effectiveness parameter is not suitable for making heat-shield designs, it is useful in comparing various materials subjected to similar test environments or in investigating the effect of changes in environment on a particular material.

The combined effect of density and composition on the effectiveness of phenolic-nylon ablation materials is shown in figure 3. The trend is for the effectiveness to decrease with increasing density; however, the extent of the effect of density varied with the material considered.

The effectiveness values do not provide a complete indication of the usefulness of a material since the machining characteristics of a material and the physical integrity of the char developed during testing are considered to be important to the selection of a particular material. For example, the material with a density of 160 kg/m^3 (fig. 4) was molded without any compaction; thus the resulting model had a powdery texture and was fragile and difficult to handle. On the other hand, the model having a density of 320 kg/m^3

was molded so that the final mold volume was approximately 50 percent of the bulk volume, and the resulting model had a firm texture and was easily machined. The appearance of the charred material, shown in figure 4, indicates that the physical characteristics of the char of the lower density model are inferior to those of the higher density model. The physical characteristics of the chars improved as the density increased, a substantial improvement occurring as the density increased from 160 kg/m^3 to 230 kg/m^3. The appearance of the chars for various densities of the material composed of 20 percent phenolic, 20 percent nylon, and 60 percent Microballoons is characteristic of the chars developed for different densities of each of the other phenolic-nylon materials; that is, the characteristics of the char improve with density and the chars have a columnar structure that extends through the depth of the char. The spacing between the columns of material tends to increase as the density decreases and this phenomenon accounts for the weaker char structure.

Part of the effectiveness variations shown in figure 3 was due to variations in composition. As the mass percentage of Microballoons was increased while the ratio of nylon to phenolic powder was kept 1 to 1, the effectiveness increased as shown in figure 5. Furthermore, the composites that were molded so that the mold volume was 70 percent of the bulk volume had the highest ablative effectiveness. The data points for each composite represent different density moldings. This is accomplished by varying the ratio of mold volume to bulk volume. The effectiveness curve is a least-squares fit for all data points. A similar plot is shown in figure 6 where the percentage of Microballoons remains constant while the percentages of phenolic powder and nylon were varied. The effectiveness increased as the percentage of nylon was increased. Although figures 5 and 6 show the effectiveness to increase monotonically as the percentage of Microballoons or nylon increases, the optimum composition cannot be selected solely on the basis of ablative effectiveness, but char integrity must also be considered. Consequently, the results shown in figures 5 and 6 are useful only in that they show the effect of material composition on ablative effectiveness.

A 560 kg/m^3 ablator (model 27) that has been evaluated extensively (ref. 9) was tested at the same condition as the low-density materials listed in table I. The effectiveness E of some of the low-density materials was 1.5 times greater than that of the 560 kg/m^3 material at a cold-wall heating rate of 0.23 MW/m^2. However, the physical integrity of the high-density char (fig. 7) was superior to that of the low-density chars.

Effect of Honeycomb

Since a honeycomb matrix is commonly used to improve the physical integrity of the char of ablation materials, a model (model 25, table I) which contained a 56 kg/m^3 phenolic-glass honeycomb matrix was tested. The ablative effectiveness E of the honeycomb-supported material was equivalent (table I) to that of the material of the

same density without the honeycomb (model 21). Furthermore, the physical appearance and integrity of the char (fig. 8) were improved significantly as evidenced by no spalling and less surface recession.

Material Performance for Various Test Conditions

After completion of the tests to determine the effect of variations in density and composition, one ablation material was selected and its performance was determined at various test conditions. The particular material selected for additional testing (30 percent phenolic, 10 percent nylon, and 60 percent phenolic Microballoons, with a phenolic-glass honeycomb matrix) was one with high ablative effectiveness and good char integrity. The nominal density of the material including the honeycomb matrix was 220 kg/m^3. The density of the honeycomb was 42 kg/m^3. The results of the tests conducted for this material and the test conditions are listed in table II.

The performance of the 30-10-60 material on the basis of ablative effectiveness is shown in figure 9, where the effectiveness is plotted as a function of cold-wall heating rate for various stagnation pressures and test-stream oxygen concentration. The two effectiveness curves are least-squares fits for the data points resulting from the tests made in test streams containing oxygen concentrations of 3 and 23 percent. The trend is for the effectiveness to increase with increased heating rate. For comparable heating rates, the effectiveness of the material tested in a test stream containing an oxygen concentration of 23 percent was about 73 percent of the effectiveness of the tests made in a test stream containing an oxygen concentration of 3 percent. The increase in effectiveness with heating rate and decrease in effectiveness with oxygen concentration shown in figure 9 are consistent with results obtained from studies of higher density phenolic-nylon ablators (ref. 10).

The effects of the test environment are also evident from the appearance of the charred models (fig. 10). In general, the physical integrity of the char was good in that it remained in place during the test for all test conditions. The most obvious effect on the char was the test-stream oxygen concentration as shown in figures 10(d) and 10(i). For the models tested in a 3-percent-oxygen test stream, the surface recession was negligible; however, for the models tested in a 23-percent-oxygen test stream, the surface recession was from 0.51 to 0.64 cm.

ANALYSIS OF ABLATIVE MASS REQUIREMENTS

As part of the study of low-density phenolic-nylon ablators, an analysis was made to determine the mass requirements for the ablative heat shield of an approximate configuration of a manned lifting-body entry vehicle. The heat-shield mass requirements were determined for phenolic-nylon ablators with densities of 220 and 580 kg/m^3.

Entry-Body Configuration

Since local heating effects were to be considered in determining the heat-shield mass requirements, an entry-body configuration was selected on the basis of amenability to calculation of local heating and aerodynamic behavior. The selection was also made with the intention of selecting a configuration that could be considered a reasonable approximation of a manned lifting-body entry vehicle. The configuration selected, shown in figure 11, is one-half of a 13° half-angle cone with a spherically blunt tip having a radius of 0.43 m. The vehicle has a length of 8.53 m and a total mass of 5500 kg. The selected body configuration approximates some of the present manned lifting-body entry vehicles. For example, the M-2 lifting body was evolved from one-half of a 13° half-angle cone with a spherically blunt tip (ref. 11).

Aerodynamic Characteristics

The aerodynamic-force coefficients, lift and drag, were calculated for the blunted half-cone from Newtonian theory from reference 12. The results of these calculations are shown in figure 12 where L/D and C_L are plotted as functions of angle of attack. The angle-of-attack variation considered in this analysis (1° to 40°) provided aerodynamic-force coefficients over the range from approximately $(L/D)_{max}$ to $(C_L)_{max}$.

Trajectories

Four constant-altitude trajectories describing the flight environment for the blunt half-cone vehicle at values of L/D of 0.67, 0.93, 1.49, and 2.1 were generated. These L/D values correspond, respectively, to angles of attack of 40°, 30°, 15°, and 1°. For the trajectories considered in this analysis, entry was assumed to start at an altitude of 122 km, an initial flight-path angle of -1.5°, and an initial velocity of 7.9 km/sec.

The entry trajectories and associated heating rates for angles of attack of 1°, 15°, 30°, and 40° are illustrated in figures 13 and 14, respectively. It can be seen in figure 13 that as the angle of attack increases from that for approximately $(L/D)_{max}$ to that for $(C_L)_{max}$, entry is made at higher altitudes. The constant-altitude portion of the trajectories shown in figure 13 was obtained by roll-modulating the vehicle about the velocity vector while maintaining a constant angle of attack.

Heat-Transfer Distributions

For the present analysis, theoretical and empirical methods were used to determine the stagnation-point heating on the spherical nose and the local heating on the afterbody as some fraction of the stagnation heating. The laminar stagnation-heating-rate correlation of reference 13, which contains the correction for dissociation and the ratio of external to

wall enthalpy, was used in determining the stagnation heating rates shown in figure 14. The cold-wall stagnation-heating-rate correlation can be written as

$$q_s = \frac{17\,800\sqrt{\rho}\,V^{3.15}}{\sqrt{r}}$$

where ρ is the atmospheric density, V the vehicle velocity, and r the nose radius.

The ratio of local heating to that of the stagnation value was determined by using a relatively simple method (ref. 14) for computing the laminar heating over hypersonic vehicles at an angle of attack and with a highly cooled surface. This method used the "axisymmetric analog" (refs. 15 and 16) for transforming the general three-dimensional boundary-layer equations into the same form as those for an axisymmetric body at zero angle of attack and the laminar heating method of reference 17. An additional discussion of this method, including a comparison of experimental and predicted heating distributions, is found in reference 14.

The calculated heating-rate ratio q/q_s to the windward center line of the blunt half-cone is shown in figure 15 for angles of attack of 1^o, 15^o, 30^o, and 40^o. This figure shows the extent to which the heating-rate ratio increased with angle of attack for a given s/r station. The circumferential heating-rate ratios at s/r stations of 1.34 (tangent point) and 10 are shown in figure 16 for each of the four angles of attack.

Ablative Mass Requirements

The ablative mass requirements of a blunted 13^o half-cone for entry at angles of attack of 1^o, 15^o, 30^o, and 40^o were determined for two phenolic-nylon ablation materials, one having a density of 580 kg/m^3 and the other having a density of 220 kg/m^3. The ablative mass requirements were those necessary to limit the back-surface temperature rise of a substructure to 167^o K, where the heat capacity of the substructure is 4.80 $J/m^2\text{-}^oK$. The calculations were made by use of the charring-ablator program of reference 18 and the trajectory environmental conditions and the heating distributions previously discussed.

The material properties used for the 580 kg/m^3 ablator (table IV) were from reference 19 and give good agreement between calculated and experimental results. The material properties used for the 220 kg/m^3 ablator (table IV) were obtained by adjusting the thermal conductivities and densities of the charred and uncharred materials until the calculated thermal response of the low-density material was approximately that obtained experimentally. With the exception of the thermal conductivities and densities, the material properties of the 220 kg/m^3 ablator were assumed to be the same as the properties of the 580 kg/m^3 ablator. This assumption appears to be reasonable since the two ablators consist of the same material components; however, the percentages of the component

materials used were not the same for the high- and low-density ablators (table I). Even so, the need exists for thermophysical property measurements on the low-density ablators in order that more reliable inputs may be used in calculating the performance of the low-density ablators.

The environmental parameters used in the charring ablator program were stagnation cold-wall heating rates and enthalpy as functions of time along with the oxygen concentration $\left(C_e = 23 \text{ percent}\right)$. The ablative mass requirements were determined for various heating-rate ratios q/q_s with the enthalpy at the edge of the boundary layer considered to be the same as that at the stagnation point.

The calculated mass required for an ablative heat shield as a function of heating-rate ratio q/q_s for entry at angles of attack of 1^o, 15^o, 30^o, and 40^o is shown in figures 17(a) and 17(b) for the 580 and 220 kg/m^3 ablators. These results show that the entry attitude of a lifting-body entry vehicle has a significant effect on the amount of ablation material required and that for any given entry attitude the ablative mass requirement can be reduced significantly by using a 220 rather than a 580 kg/m^3 phenolic-nylon ablator.

The total mass of ablation material required was obtained by dividing the surface area into small areas, obtaining the average heating-rate ratio q/q_s for each area, obtaining the ablative mass requirement from figures 17(a) and 17(b), and summing the mass requirements of each area. The results of such approximate integrations are shown in figure 18 where the total ablative mass requirements are plotted against angle of attack. The decrease in total ablative mass requirement with increasing angle of attack is a manifestation of the lower heat loads and, in general, the lower heating rates experienced at the larger angles of attack. The effect of varying the angle of attack from that for $(L/D)_{max}$ to that for $(C_L)_{max}$ was to decrease the total mass required for an ablative heat shield by approximately 50 percent for each ablator.

The ablative mass requirement as a function of maximum longitudinal range is shown in figure 19 for the 220 and 580 kg/m^3 ablator. The ablative mass requirement increases with increasing range (decreasing angle of attack) because the total integrated heating increases with increasing range. Consequently, lower mass requirements are obtained at the expense of range capability.

When the effect of the density of the ablator on the total ablative mass requirement (fig. 18) is examined, it is apparent that an appreciable reduction in the total ablative mass requirement can be realized by reducing the density of the phenolic-nylon ablator from 580 to 220 kg/m^3. In fact, the mass requirement for the ablative heat shield of the windward surface of the lifting-body entry vehicle was reduced 34 percent by using a 220 kg/m^3 rather than a 580 kg/m^3 phenolic-nylon ablator. This mass reduction was essentially independent of the entry attitude of the lifting-body entry vehicle.

CONCLUSIONS

An experimental study was made of the ablative performance of phenolic-nylon materials having densities of 160 to 320 kg/m^3, and an analytical study was made of the potential benefits that a low-density ablator might have with respect to mass requirements for an ablative heat shield of a lifting-body entry vehicle. Results of the study lead to the following conclusions:

1. The ablative effectiveness of some of the low-density material was about 1.5 times that of a 580 kg/m^3 material when subjected to a cold-wall heating rate of 0.23 MW/m^2.

2. The trend for the low-density materials is for ablative effectiveness to decrease with increasing density.

3. The ablative effectiveness of the phenolic-nylon materials improved as the percentage of phenolic Microballoons was increased. However, the physical characteristics of the uncharred and charred materials limits the amount of Microballoons that can be used in an ablative material.

4. The ablative effectiveness of a 220 kg/m^3 material when subjected to various test conditions increased with increasing heating rates and decreased with increasing test-stream oxygen concentrations. Furthermore, the char of the 220 kg/m^3 material, supported in a phenolic-glass honeycomb, maintained good physical integrity as evidenced by no spalling for all test conditions.

5. Analysis of the mass requirements for an ablative heat shield of the windward side of one-half of a blunted 13^o half-angle cone indicates that the total mass of ablation material required to limit the back-surface temperature rise to 167^o K can be reduced by as much as 34 percent by using a 220 kg/m^3 ablator rather than a 580 kg/m^3 ablator.

6. Analysis of the effect of entry attitude on ablative mass requirements indicates that a mass reduction of approximately 50 percent can be obtained when the angle of attack is increased from that for maximum lift-drag ratio to that for maximum lift coefficient.

Langley Research Center,
National Aeronautics and Space Administration,
Langley Station, Hampton, Va., March 25, 1969,
124-08-03-18-23.

REFERENCES

1. Meltzer, J.; Slaughter, J. I.; and Sallis, D. V.: Thermal Protection System for the SV-5 (PRIME) Ablative Lifting Reentry Vehicle. SSD-TR-65-158, U.S. Air Force, Oct. 22, 1965. (Available from DDC as AD 367288.)

2. Fallis, William B.: Feasibility Study of Minimum Manned Lifting Body Entry Vehicle. Vol. I. Publication NB 66-9 (Contract No. NAS 4-840), Northrop Norair, Jan. 1966.

3. LaPorte, A. H.: Research on Refurbishable Thermostructural Panels for Manned Lifting Entry Vehicles. NASA CR-638, 1966.

4. Newell, J.: A Study of Thermo-Structural Design Concepts for Lifting Entry Vehicles. NASA CR-240, 1965.

5. Chapman, Andrew J.: An Experimental Evaluation of Three Types of Thermal Protection Materials at Moderate Heating Rates and High Total Heat Loads. NASA TN D-1814, 1963.

6. Comm. on Metric Pract.: ASTM Metric Practice Guide. NSB Handbook 102, U.S. Dep. Com., Mar. 10, 1967.

7. Moss, James N.; and Howell, William E.: Recent Developments in Low-Density Ablation Materials. Advances in Structural Composites, SAMPE Vol. 12, Soc. Aerosp. Mater. Process Eng., c.1967.

8. Swann, Robert T.; Dow, Marvin B.; and Tompkins, Stephen S.: Analysis of the Effects of Environmental Conditions on the Performance of Charring Ablators. J. Spacecraft Rockets, vol. 3, no. 1, Jan. 1966, pp. 61-67.

9. Swann, Robert T.; Brewer, William D.; and Clark, Ronald K.: Effect of Composition, Density, and Environment on the Ablative Performance of Phenolic Nylon. NASA TN D-3908, 1967.

10. Dow, Marvin B.; and Swann, Robert T.: Determination of Effects of Oxidation on Performance of Charring Ablators. NASA TR R-196, 1964.

11. Syvertson, C. A.; Swenson, B. L.; Anderson, J. L.; and Kenyon, G. C.: Some Considerations of the Performance of a Maneuverable, Lifting-Body, Entry Vehicle. Vol. 16 of Advances in the Astronautical Sciences, Norman V. Peterson, ed., Western Periodicals Co., c.1963, pp. 898-918.

12. Wells, William R.; and Armstrong, William O.: Tables of Aerodynamic Coefficients Obtained From Developed Newtonian Expressions for Complete and Partial Conic and Spheric Bodies at Combined Angles of Attack and Sideslip With Some Comparisons With Hypersonic Experimental Data. NASA TR R-127, 1962.

13. Detra, R. W.; Kemp, N. H.; and Riddell, F. R.: Addendum to "Heat Transfer to Satellite Vehicles Re-entering the Atmosphere." Jet Propulsion, vol. 27, no. 12, Dec. 1957, pp. 1256-1257.

14. DeJarnette, Fred R.: A Simplified Method for Calculating Heat Transfer Over Bodies at an Angle of Attack. Proc. of the Southeastern Symposium on Missiles and Aerospace Vehicles Sciences, Vol. 1, Amer. Astronaut. Soc., c.1966, pp. 12-1 – 12-11.

15. Cooke, J. C.: An Axially Symmetric Analogue for General Three-Dimensional Boundary Layers. R. & M. No. 3200, Brit. A.R.C., 1961.

16. Beckwith, Ivan E.: Similarity Solutions for Small Cross Flows in Laminar Compressible Boundary Layers. NASA TR R-107, 1961.

17. Lees, Lester: Laminar Heat Transfer Over Blunt-Nosed Bodies at Hypersonic Flight Speeds. Jet Propulsion, vol. 26, no. 4, Apr. 1956, pp. 259-269, 274.

18. Swann, Robert T.; Pittman, Claud M.; and Smith, James C.: One-Dimensional Numerical Analysis of the Transient Response of Thermal Protection Systems. NASA TN D-2976, 1965.

19. Brewer, William D.; Stroud, C. W.; and Clark, Ronald K.: Effect of the Chemical State of Pyrolysis Gases on Heat-Shield Mass. NASA TN D-4975, 1968.

TABLE I.- SUMMARY OF TEST RESULTS FOR VARIOUS PHENOLIC-NYLON MATERIALS

[q = 0.23 MW/m^2; p_t = 0.04 atm; H_e = 4.0 MJ/kg; test gas, 3 percent O_2 and 97 percent N_2]

Model	Composition, percentage by mass			Density, kg/m^3	Time for 167° K rise, sec	E, MJ/kg
	Phenolic	Nylon	Microballoons			
1	10	10	80	165	148	22.3
2	10	10	80	190	173	23.2
3	10	10	80	220	178	19.5
4	15	15	70	200	200	23.9
5	15	15	70	230	195	21.1
6	20	20	60	160	120	18.3
7	20	20	60	200	185	19.9
8	20	20	60	230	194	20.6
9	20	20	60	260	222	16.9
10	20	20	60	320	228	16.5
11	25	25	50	230	171	21.8
12	25	25	50	280	192	19.9
13	30	30	40	260	211	19.5
14	30	30	40	310	209	15.8
15	35	35	30	250	188	19.0
16	35	35	30	320	233	17.9
17	40	0	60	210	149	17.9
18	40	0	60	230	129	16.0
19	40	0	60	260	152	13.9
20	30	10	60	190	143	18.1
21	30	10	60	240	150	14.8
22	30	10	60	280	140	12.5
23	30	10	60	210	174	19.5
24	30	10	60	210	148	20.4
[a]25	30	10	60	240	144	15.3
26	10	30	60	230	198	20.2
27	25	40	35	560	272	14.4

[a]Material was in a phenolic-glass honeycomb.

TABLE II.- SUMMARY OF TEST CONDITIONS AND TEST RESULTS FOR A 220 kg/m^3 PHENOLIC-NYLON ABLATOR

[30 percent phenolic powder, 10 percent nylon, and 60 percent phenolic Microballoons, in a phenolic-glass honeycomb]

Model	q, MW/m^2	H_e, MJ/kg	p_t, atm	C_e, percent	Time for 167^o K rise, sec	Density, kg/m^3	E, MJ/kg
Apparatus B							
28	0.68	5.3	0.200	3	89	220	27.8
29	.52	4.2	.196	3	91	210	23.2
30	.93	7.2	.195	3	66	210	30.2
31	.42	4.4	.106	3	128	220	25.1
32	.70	7.7	.098	3	109	220	34.8
33	.24	3.7	.058	3	164	230	17.2
34	.36	5.3	.050	3	124	240	18.8
35	.45	7.0	.048	3	118	220	24.4
36	.54	8.4	.050	3	106	210	28.1
Apparatus D							
37	0.75	11.6	0.042	23	65	220	22.3
38	1.41	20.4	.047	23	50	230	32.0
39	1.59	22.0	.050	23	51	210	39.4
40	1.76	23.0	.053	23	45	200	39.4

TABLE III.- OPERATIONAL PARAMETERS OF TEST FACILITIES

Operational parameters	Apparatus B[a]	Apparatus D[b]
Total enthalpy, MJ/kg	1.7 to 10.4	9.3 to 37.1
Stagnation pressure, atm	0.04 to 0.4	0.02 to 0.06
Cold-wall heating rate, $MW/m^{1.5}$	0.06 to 0.44	0.19 to 0.94
Mass flow rate, kg/sec	0.045 to 0.454	0.004 to 0.022
Run time, sec	100 to 500	Continuous
Model body diameter, cm	7.60	7.60
Power level, MW	0.25 to 5	0.06 to 1.2
Mach number	3.4 to 4.3	3.2 to 3.4

[a]A 9.65° conical nozzle with a 3.8-cm-diameter throat and a 15.2-cm-diameter exit.

[b]A 8.18° conical nozzle with a 2.5-cm-diameter throat and a 10.2-cm-diameter exit.

TABLE IV.- MATERIAL PROPERTIES OF 220 AND 580 kg/m^3

PHENOLIC-NYLON ABLATORS

Uncharred material properties	220 kg/m^3 material	580 kg/m^3 material
Density, kg/m^3	220	580
Effective heat of pyrolysis, MJ/kg	1.3	1.3
Specific heat of gaseous products of pyrolysis, kJ/kg-^{o}K, at –		
260^o K	2.64	2.64
340^o K	3.86	3.86
440^o K	6.32	6.32
540^o K	11.96	11.96
640^o K	17.36	17.36
740^o K	16.36	16.36
840^o K	8.96	8.96
950^o K	6.21	6.21
1140^o K	4.93	4.93
1260^o K	4.64	4.64
1670^o K	4.21	4.21
1940^o K	4.11	4.11
Specific heat, kJ/kg-^{o}K, at –		
300^o K	1.51	1.51
370^o K	1.75	1.75
420^o K	2.00	2.00
480^o K	2.25	2.25
530^o K	2.50	2.50
590^o K	2.75	2.75
640^o K	2.97	2.97
700^o K	3.10	3.10
Thermal conductivity, W/m-^{o}K, at –		
300^o K	0.067	0.079
390^o K	0.085	0.083
500^o K	0.107	0.087
610^o K	0.130	0.090
710^o K	0.138	0.092
830^o K	0.174	0.156

TABLE IV.- MATERIAL PROPERTIES OF 220 AND 580 kg/m^3

PHENOLIC-NYLON ABLATORS – Concluded

Charred material properties	220 kg/m^3 material	580 kg/m^3 material
Density, kg/m^3	135.0	272.0
Emissivity	0.8	0.8
Heat of combustion of char, MJ/kg	10.0	10.0
Specific heat, kJ/kg-^oK, at –		
300^o K	1.63	1.63
810^o K	1.63	1.63
1370^o K	2.18	2.18
1920^o K	2.18	2.18
Thermal conductivity, W/m-^oK, at –		
300^o K	0.06	0.16
530^o K	0.11	0.16
810^o K	0.21	0.16
1090^o K	0.36	0.50
1640^o K	0.73	0.87
2200^o K	1.25	3.74

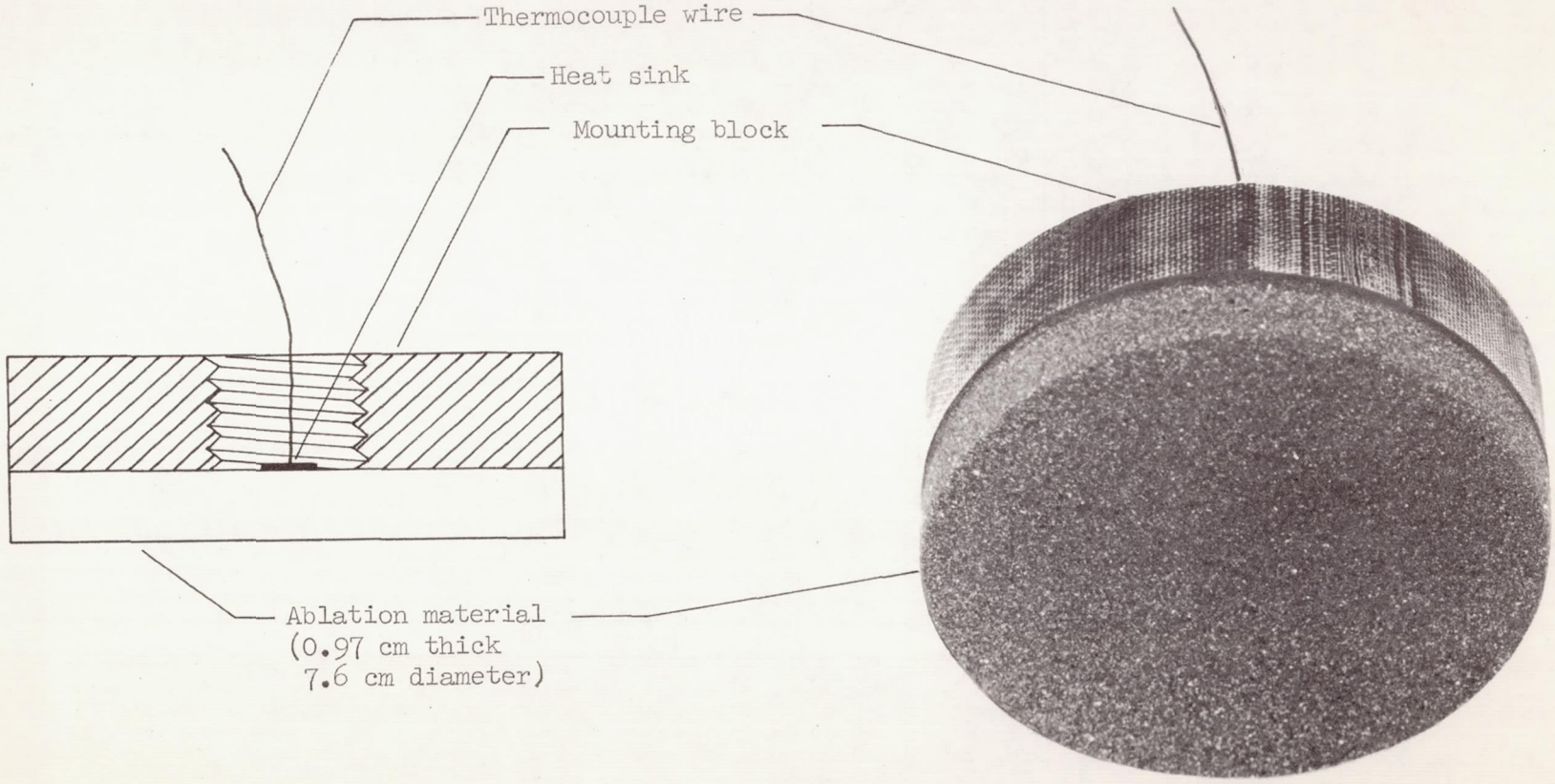

Figure 1.- Instrumentation and model configuration.

L-69-1341

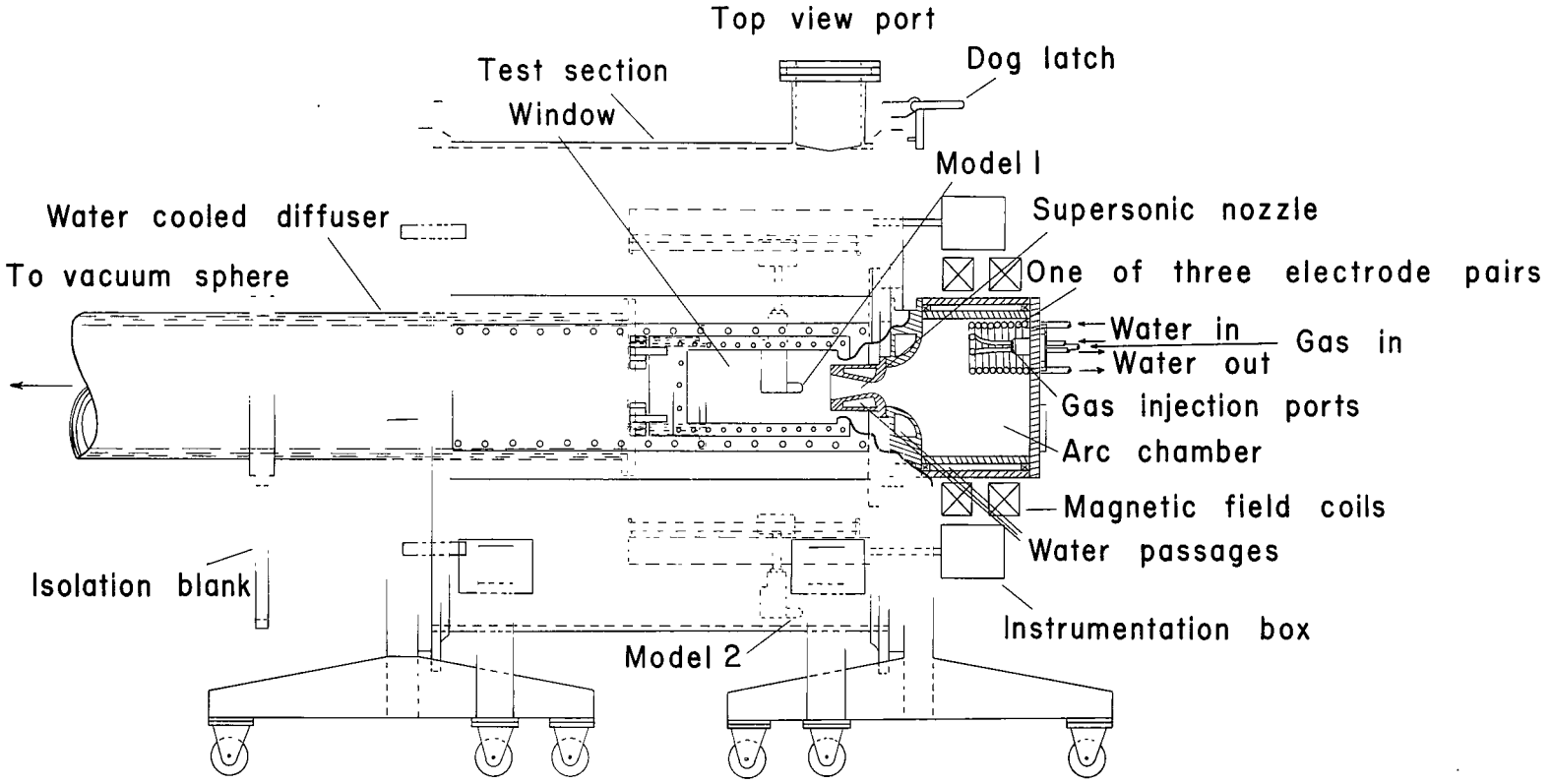

Figure 2.- Schematic diagram of Apparatus B.

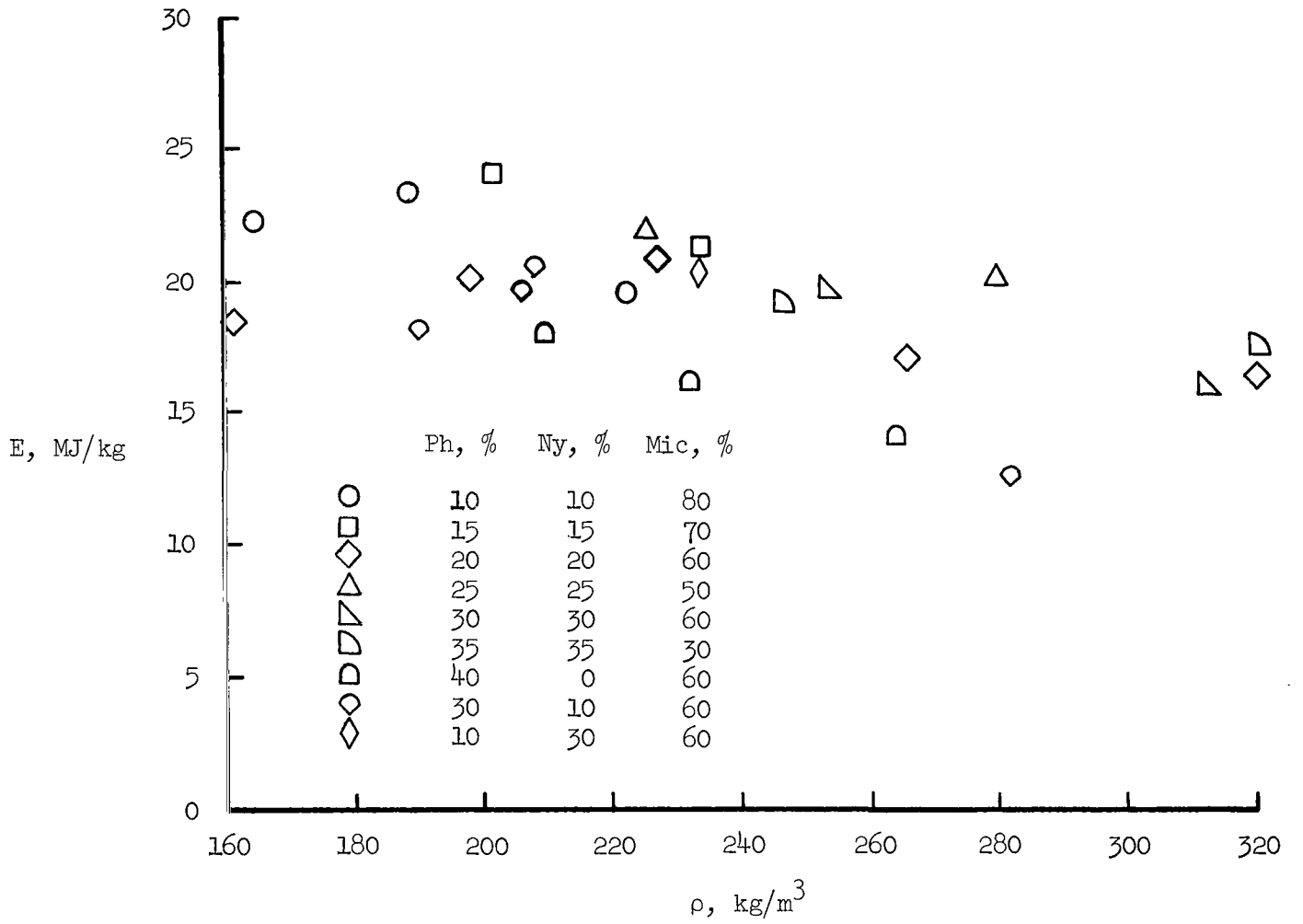

Figure 3.- Combined effect of density and composition on ablative effectiveness of phenolic-nylon composites. (The abbreviation Ph denotes powdered phenolic resin; Ny, powdered nylon; Mic, phenolic Microballoons.)

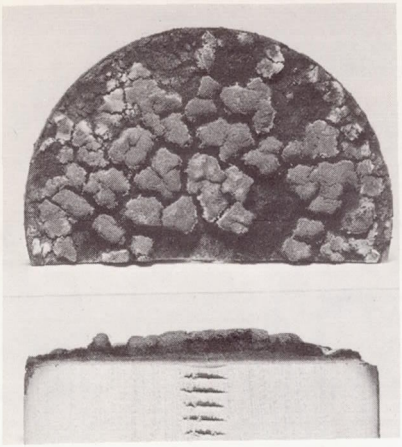

Model 6

ρ = 160 kg/m^3

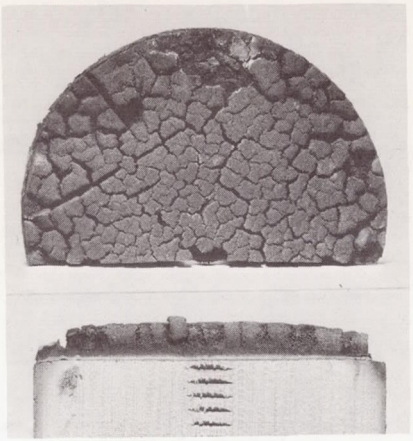

Model 7

ρ = 200 kg/m^3

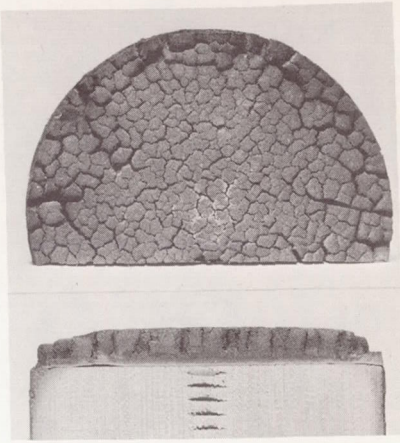

Model 8

ρ = 230 kg/m^3

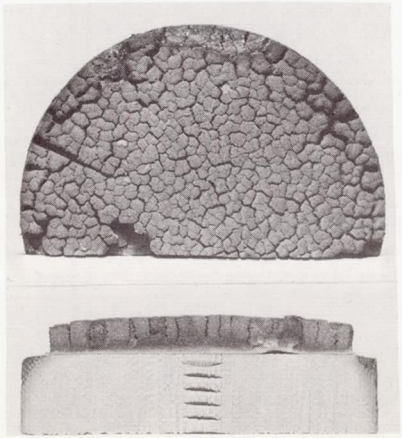

Model 9

ρ = 270 kg/m^3

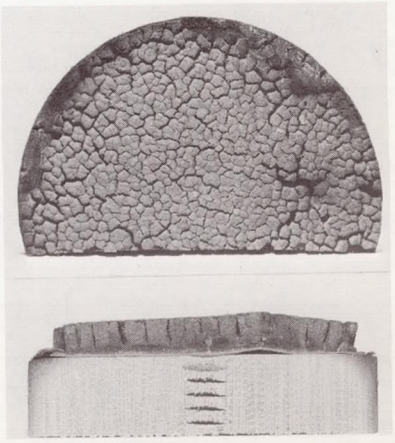

Model 10

ρ = 320 kg/m^3

L-69-1342

Figure 4.- Surface and cross-sectional views of several models after testing. The models were composed of 20 percent phenolic, 20 percent nylon, and 60 percent Microballoons, but had different densities.

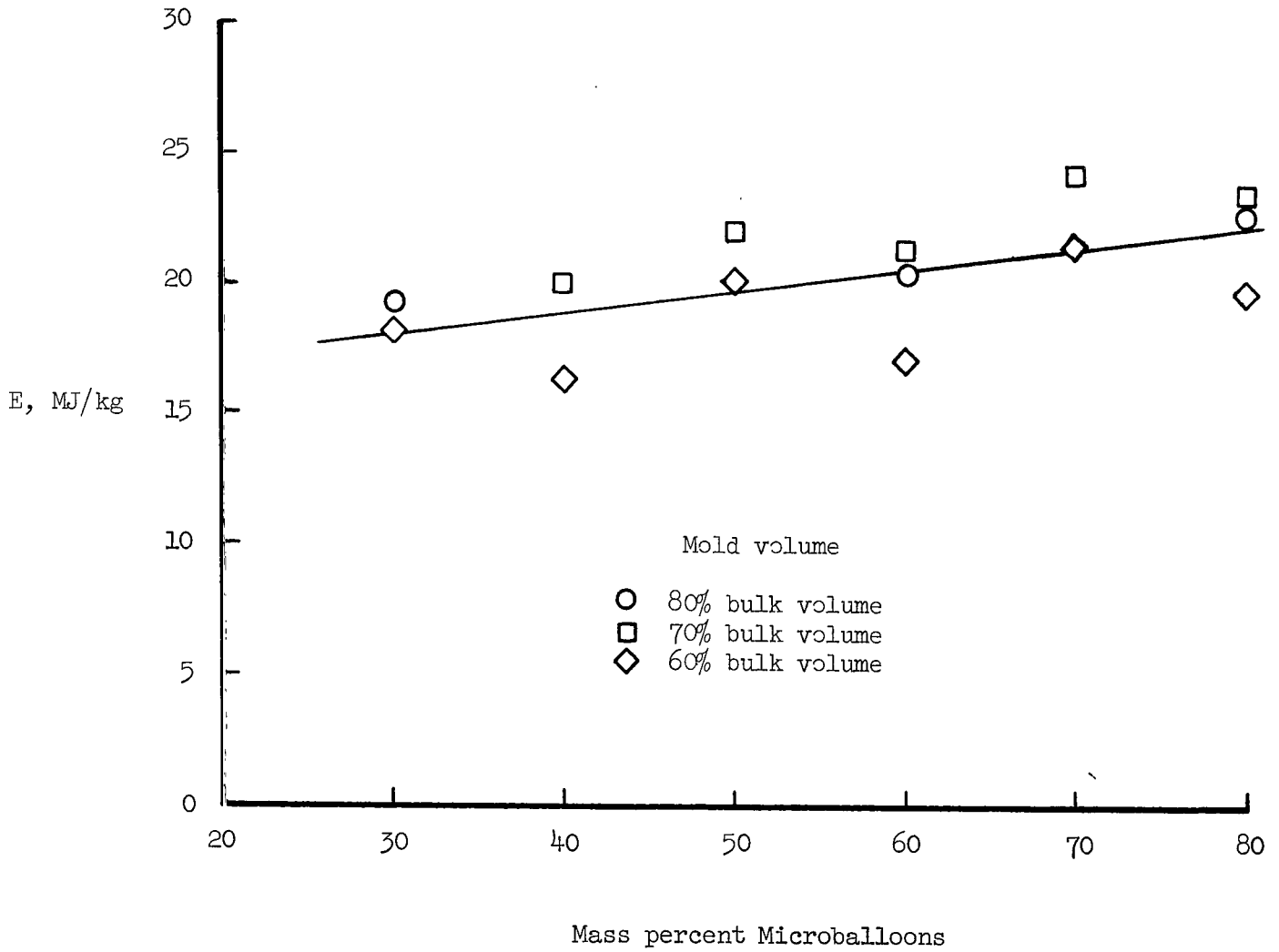

Figure 5.- Effect of phenolic Microballoon content on ablative effectiveness (1 to 1 ratio of nylon to phenolic resin).

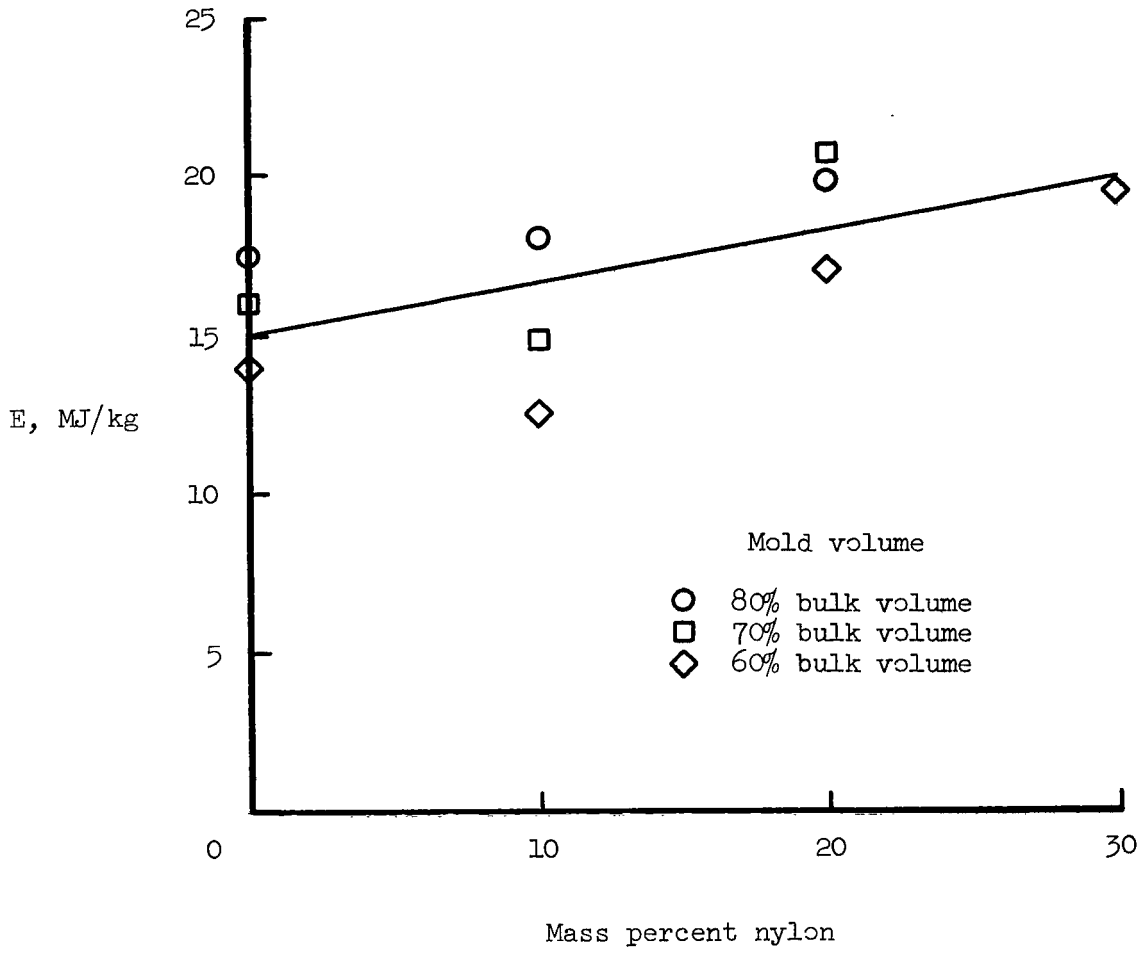

Figure 6.- Effect of nylon content on ablative effectiveness (60 percent phenolic Microballoons).

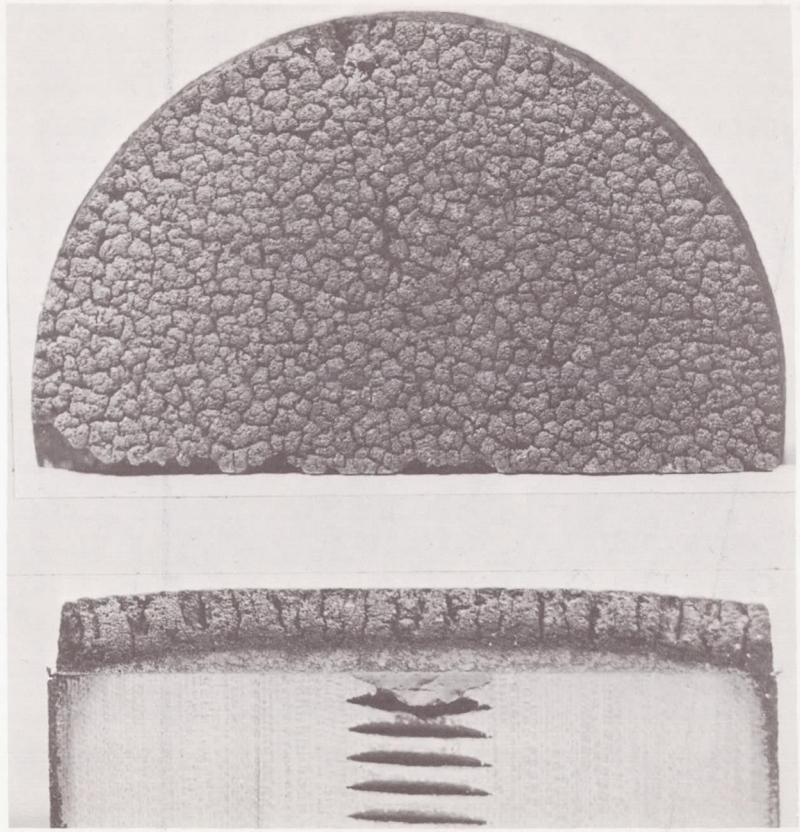

Model 27
ρ = 560 kg/m^3

L-69-1343

Figure 7.- Surface and cross-sectional views of model 27 after testing. Model composition: 25 percent phenolic, 40 percent nylon, and 35 percent Microballoons.

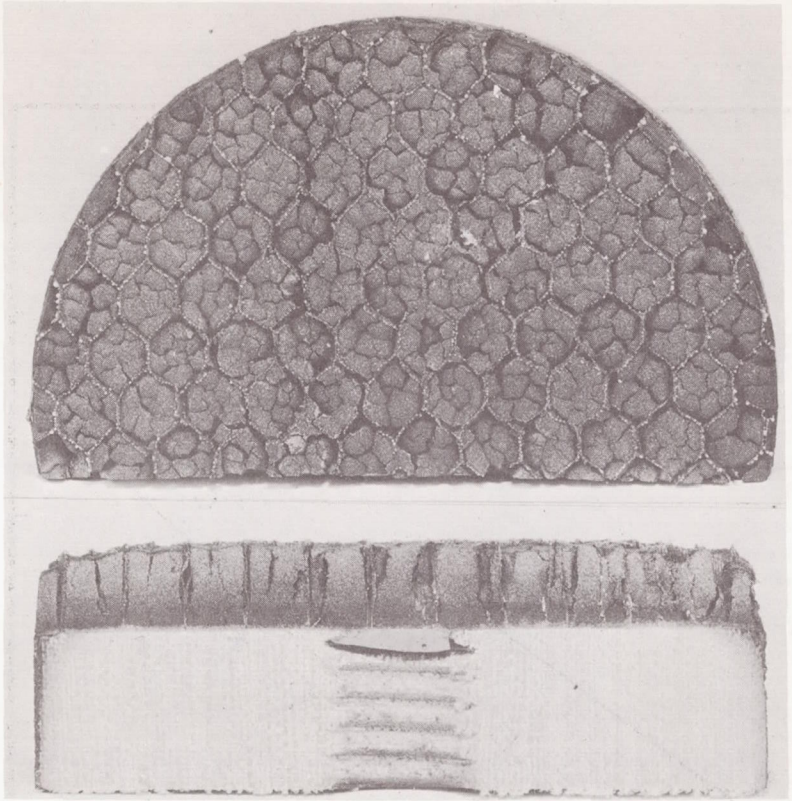

Model 25
ρ = 240 kg/m^3

L-69-1344

Figure 8.- Surface and cross-sectional views of model 25 after testing. Model composition: 30 percent phenolic, 10 percent nylon, and 60 percent Microballoons in a 56 kg/m^3 phenolic-glass honeycomb.

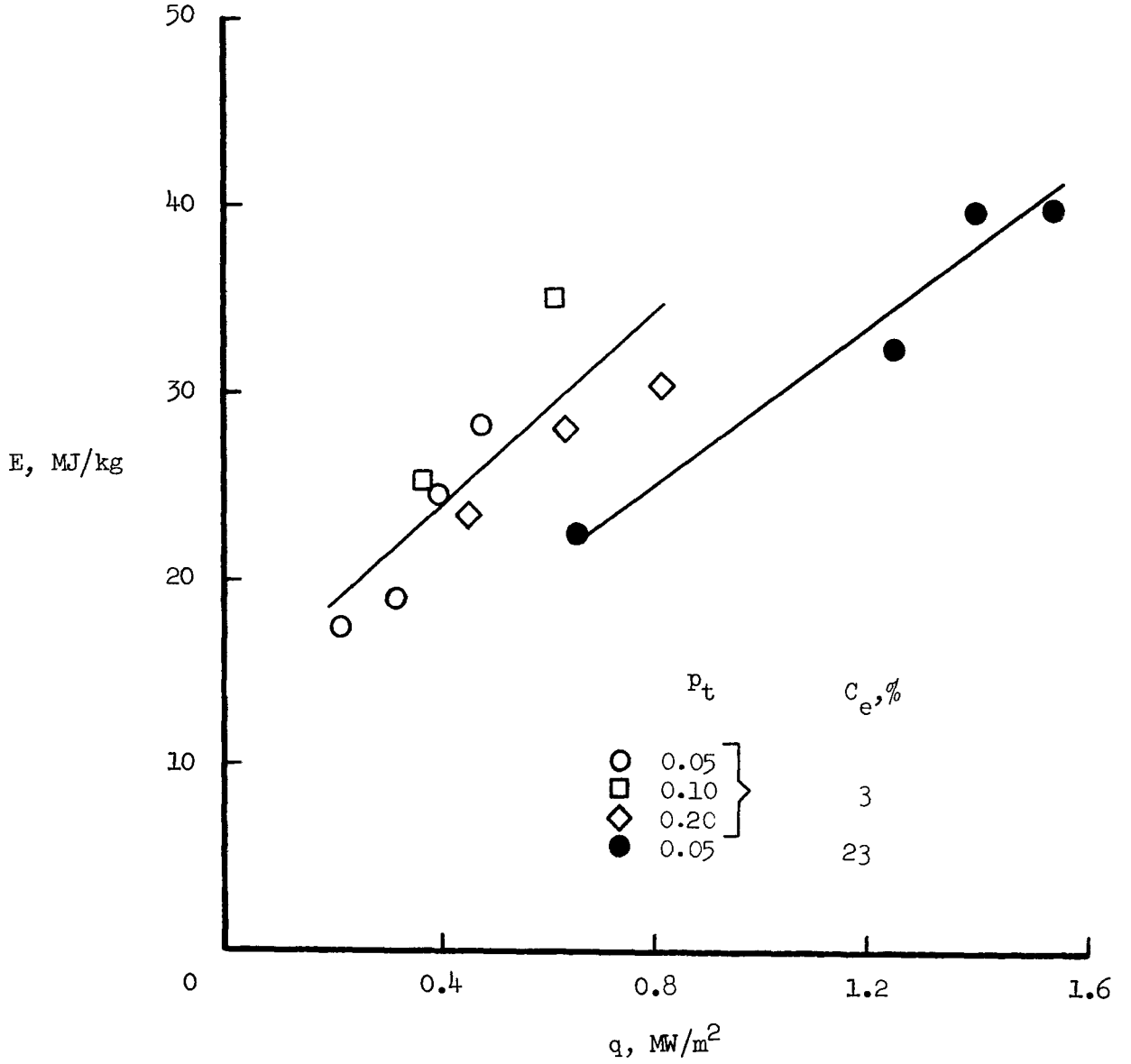

Figure 9.- Ablative effectiveness of material composed of 30 percent phenolic, 10 percent nylon, and 60 percent Microballoons as a function of heating rate. ρ = 220 kg/m^3.

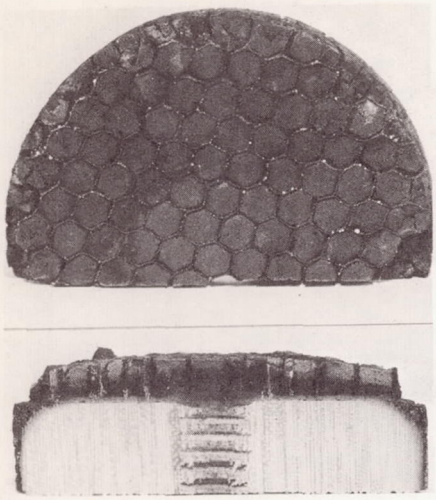

(a) Model 29. $q \approx 0.52$ MW/m^2; $C_e = 3$ percent; $H_e = 4.18$ MJ/kg; $p_t = 0.196$ atm.

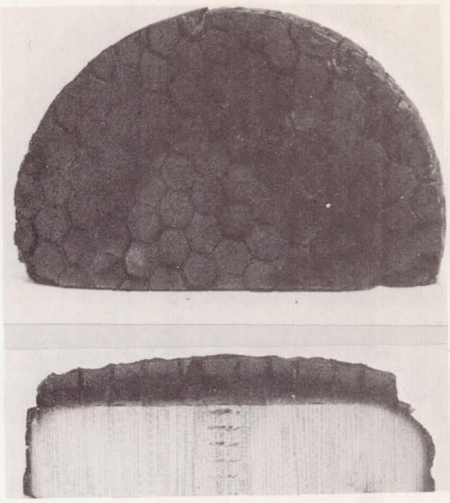

(b) Model 30. $q = 0.93$ MW/m^2; $C_e = 3$ percent; $H_e = 7.19$ MJ/kg; $p_t = 0.195$ atm.

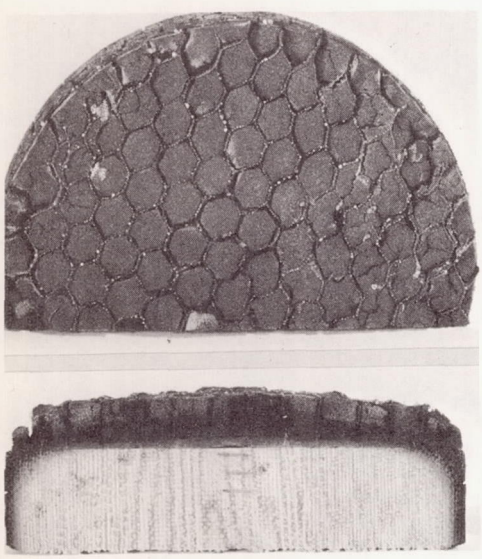

(c) Model 31. $q = 0.42$ MW/m^2; $C_e = 3$ percent; $H_e = 4.41$ MJ/kg; $p_t = 0.106$ atm.

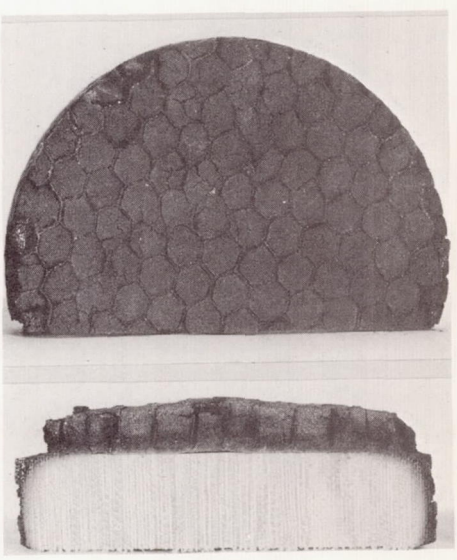

(d) Model 32. $q = 0.70$ MW/m^2; $C_e = 3$ percent; $H_e = 7.66$ MJ/kg; $p_t = 0.098$ atm.

L-69-1345

Figure 10.- Surface and cross-sectional views of various models after testing. The models were composed of 30 percent phenolic, 10 percent nylon, and 60 percent Microballoons.

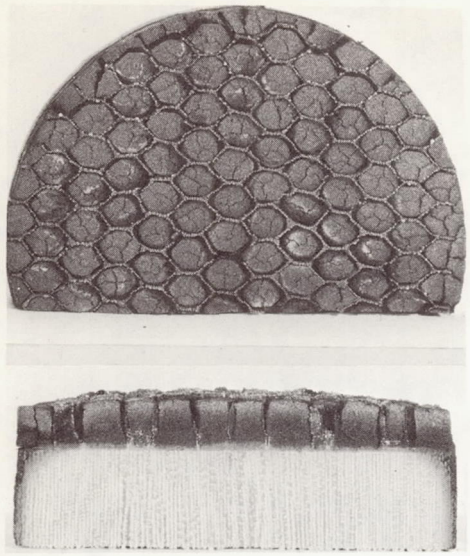

(e) Model 33. $q = 0.24\ MW/m^2$; $C_e = 3$ percent; $H_e = 3.71\ MJ/kg$; $p_t = 0.058$ atm.

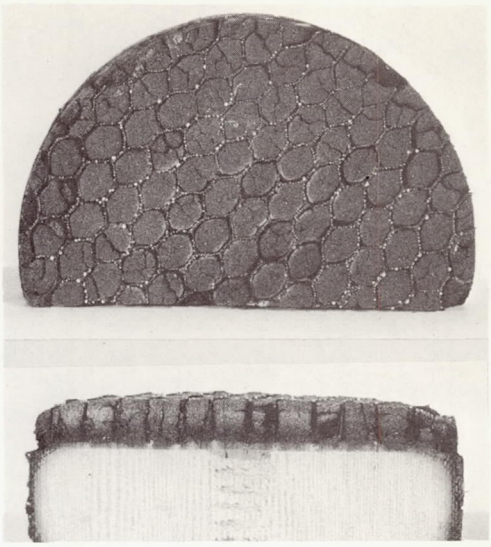

(f) Model 34. $q = 0.36\ MW/m^2$; $C_e = 3$ percent; $H_e = 5.34\ MJ/kg$; $p_t = 0.050$ atm.

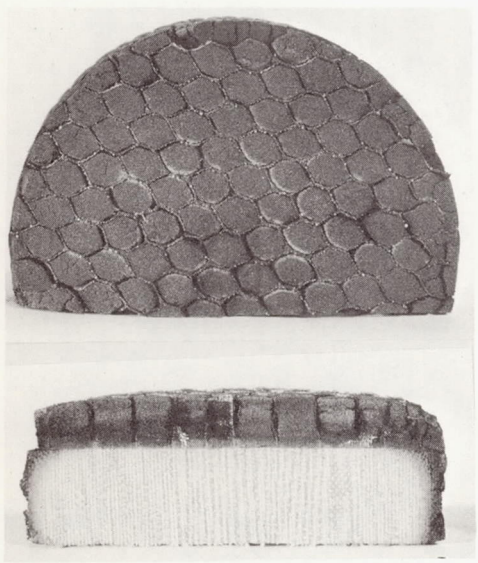

(g) Model 35. $q = 0.45\ MW/m^2$; $C_e = 3$ percent; $H_e = 6.96\ MJ/kg$; $p_t = 0.048$ atm.

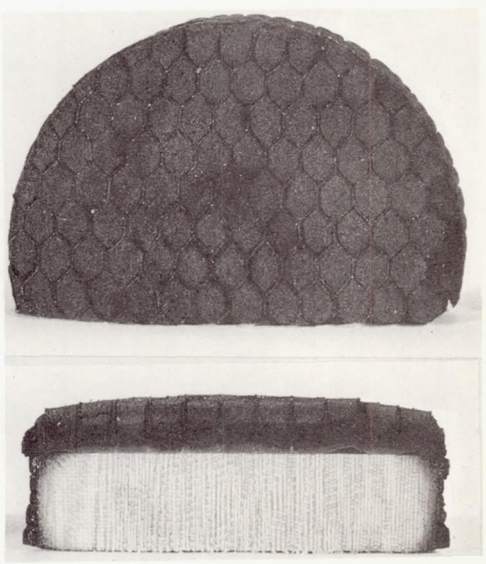

(h) Model 36. $q = 0.54\ MW/m^2$; $C_e = 3$ percent; $H_e = 8.35\ MJ/kg$; $p_t = 0.050$ atm.

Figure 10.- Continued.

L-69-1346

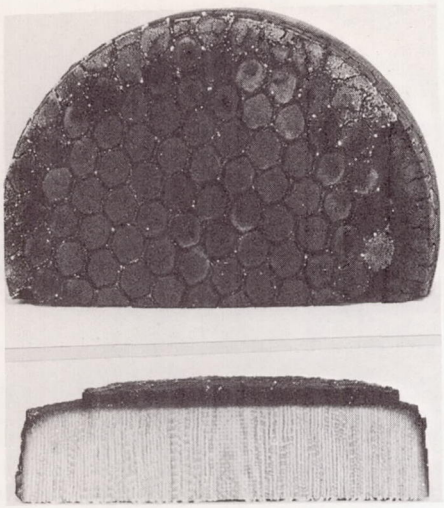

(i) Model 37. $q = 0.75\ MW/m^2$; $C_e = 23$ percent; $H_e = 11.6\ MJ/kg$; $p_t = 0.042$ atm.

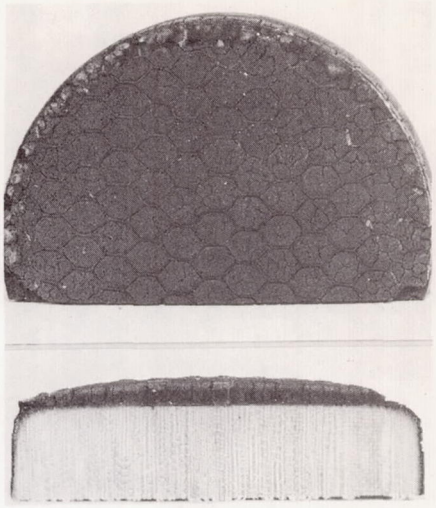

(j) Model 38. $q = 1.41\ MW/m^2$; $C_e = 23$ percent; $H_e = 20.4\ MJ/kg$; $p_t = 0.047$ atm.

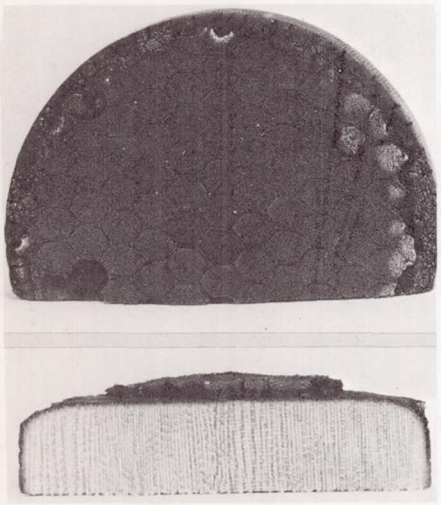

(k) Model 39. $q = 1.59\ MW/m^2$; $C_e = 23$ percent; $H_e = 22.0\ MJ/kg$; $p_t = 0.050$ atm.

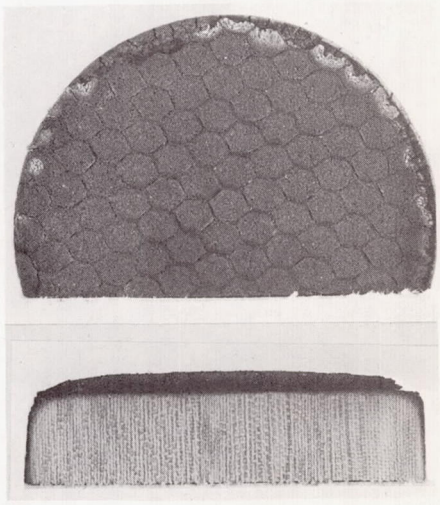

(l) Model 40. $q = 1.76\ MW/m^2$; $C_e = 23$ percent; $H_e = 23.2\ MJ/kg$; $p_t = 0.053$ atm.

Figure 10.- Concluded. L-69-1347

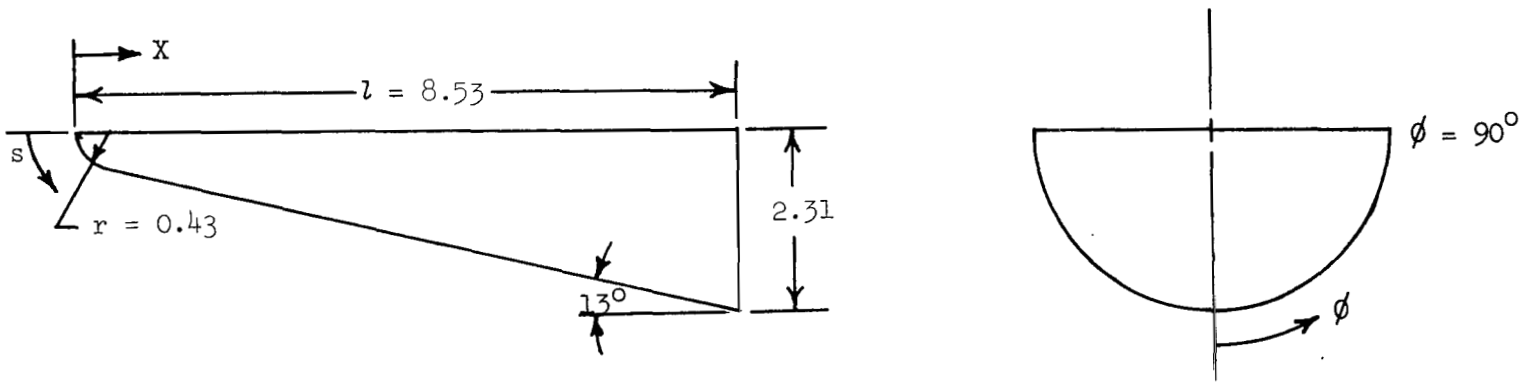

Figure 11.- Entry body configuration for which ablative mass requirements were determined. All dimensions are in meters.

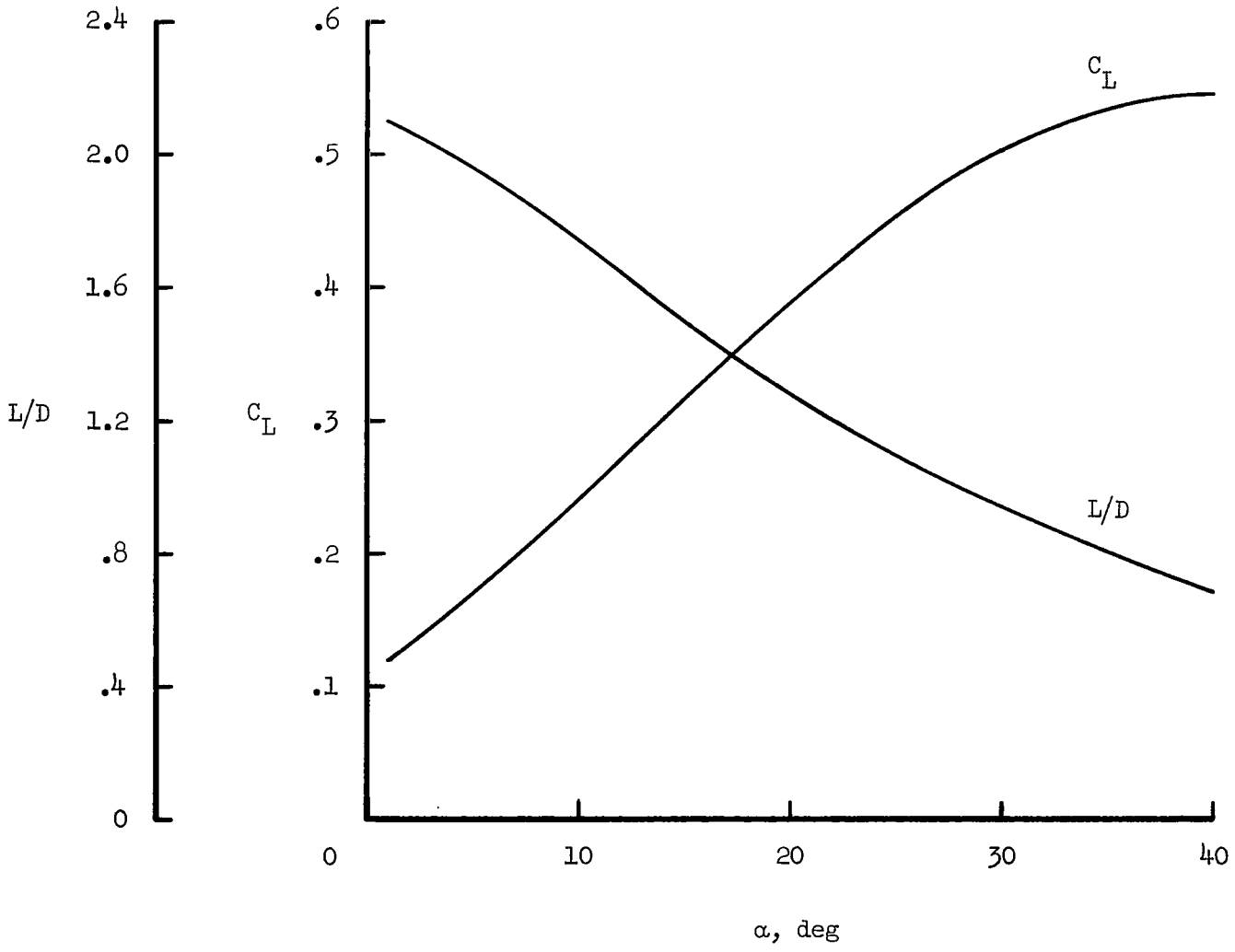

Figure 12.- Aerodynamic characteristics of 13^0 blunted half-cone.

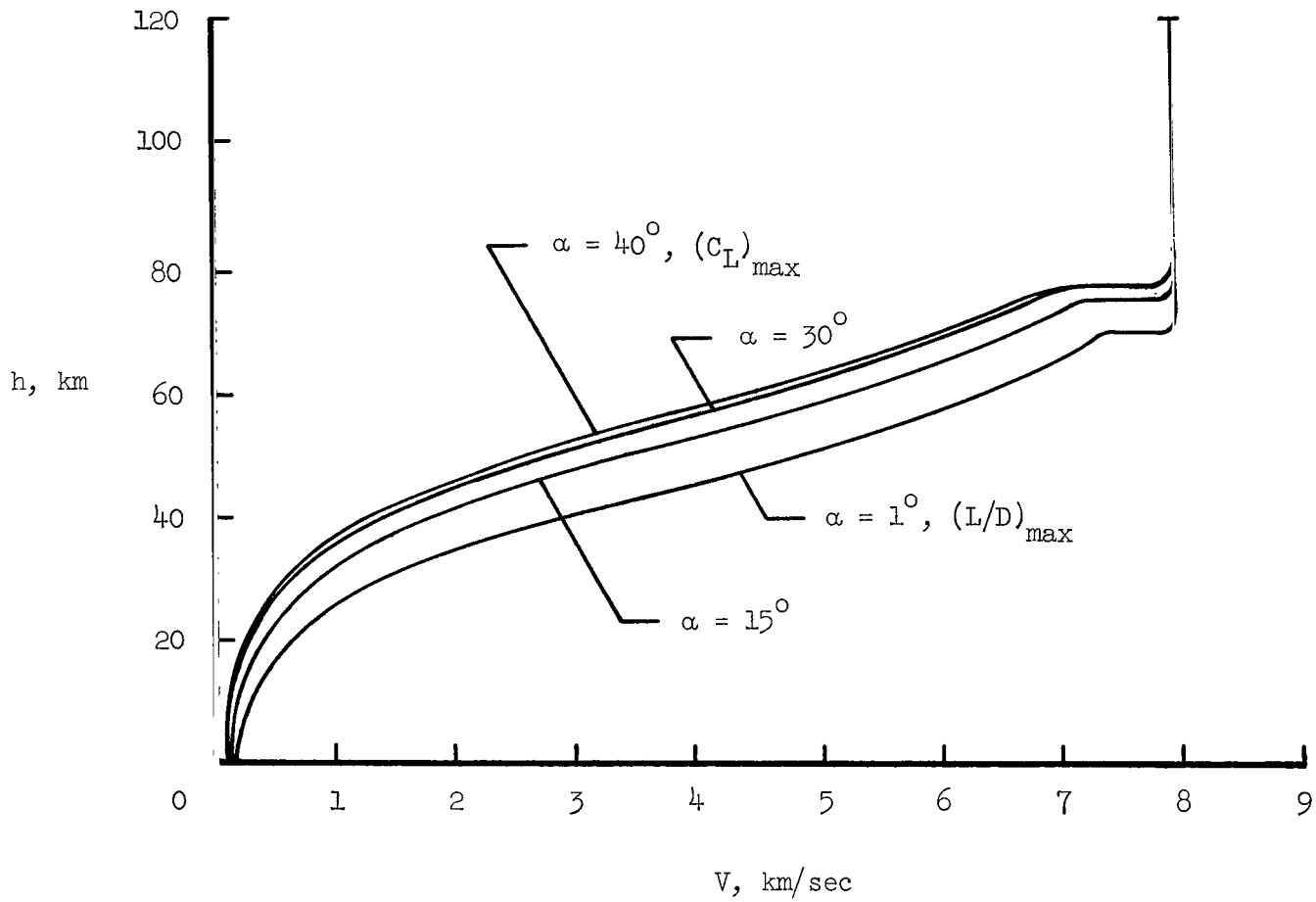

Figure 13.- Entry trajectories of 13° blunted half-cone. V_0 = 7.9 km/sec; γ_0 = -1.5°.

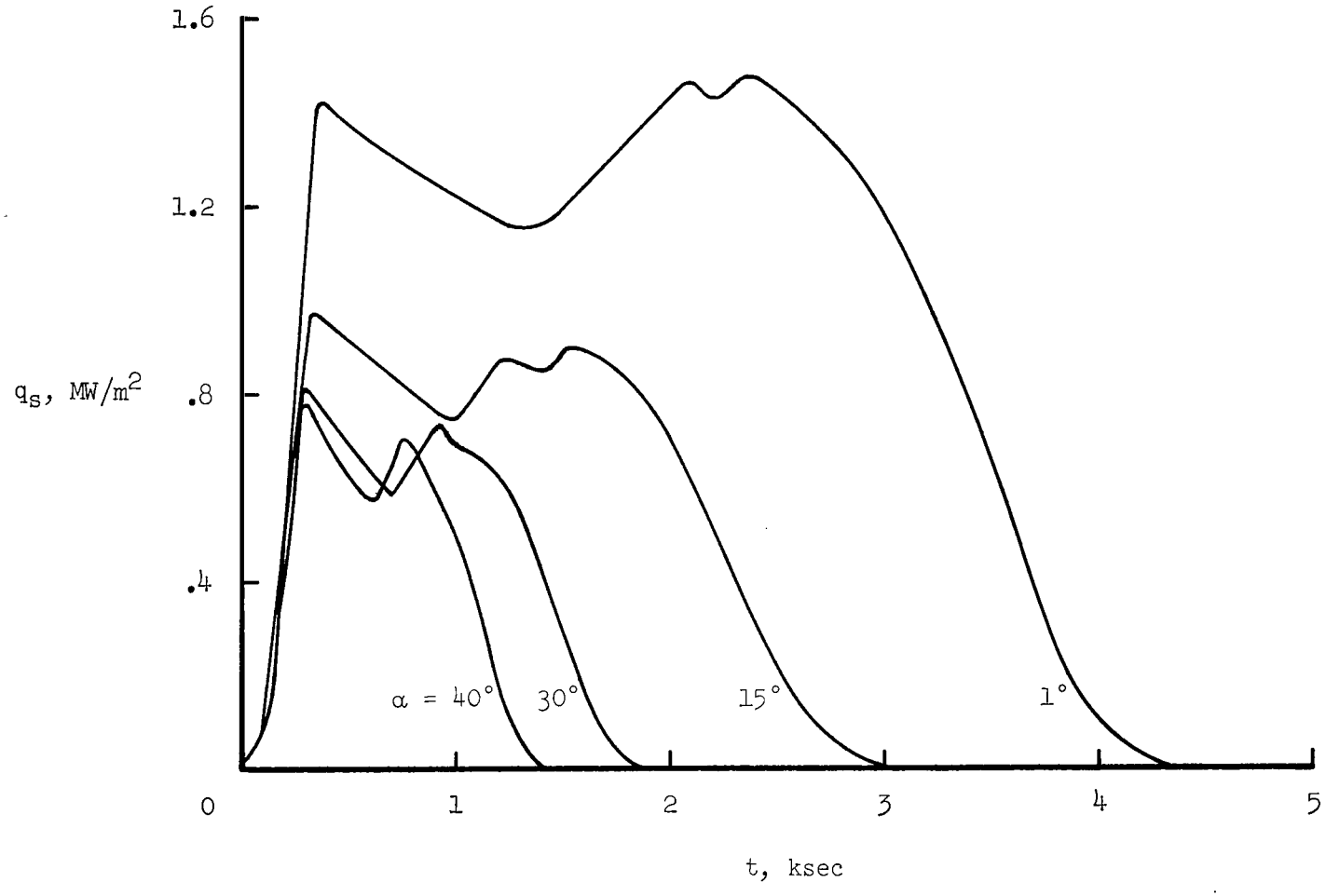

Figure 14.- Stagnation heating rates for various entry attitudes.

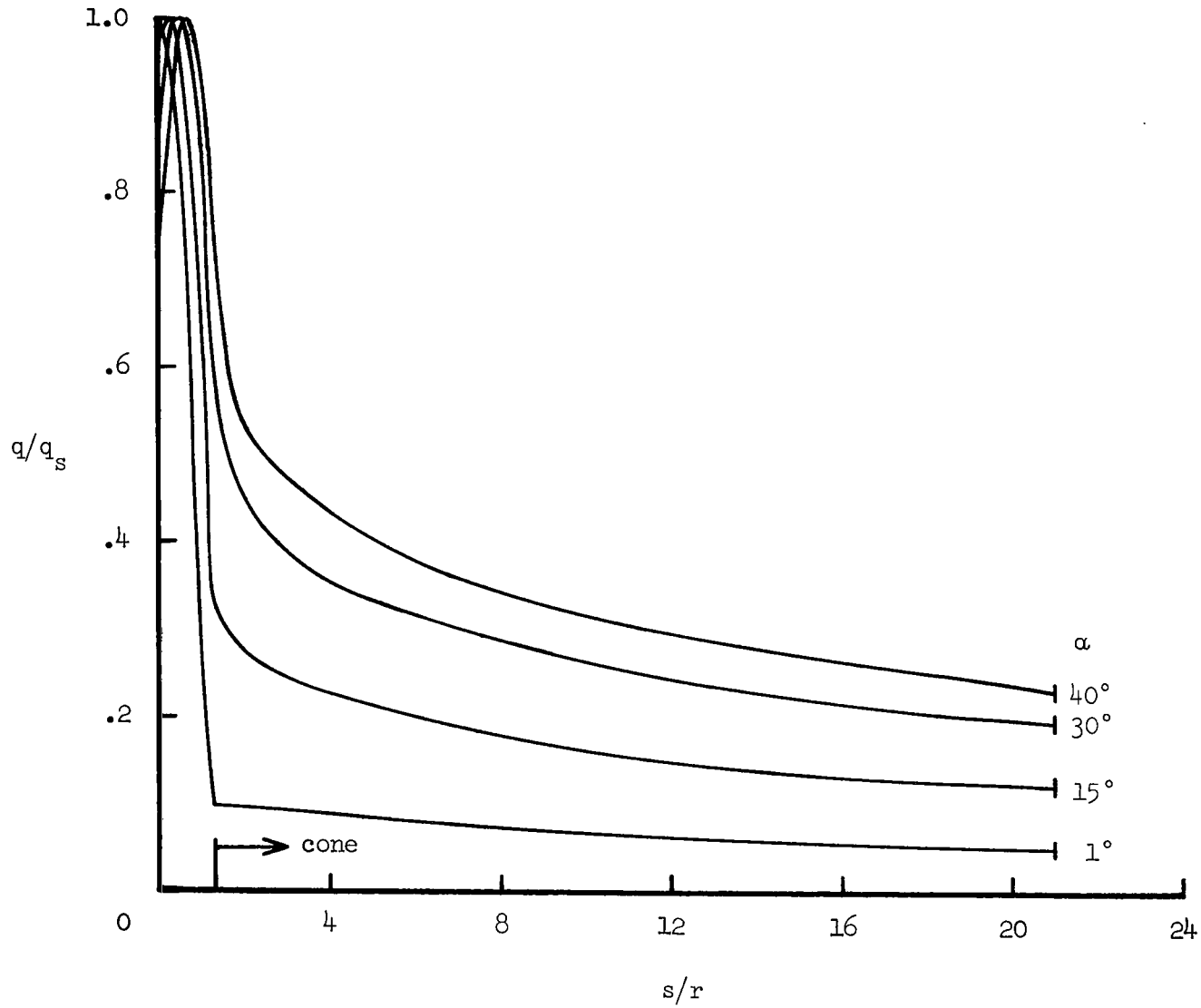

Figure 15.- Laminar heating distribution along windward center line of 13^0 blunted half-cone.

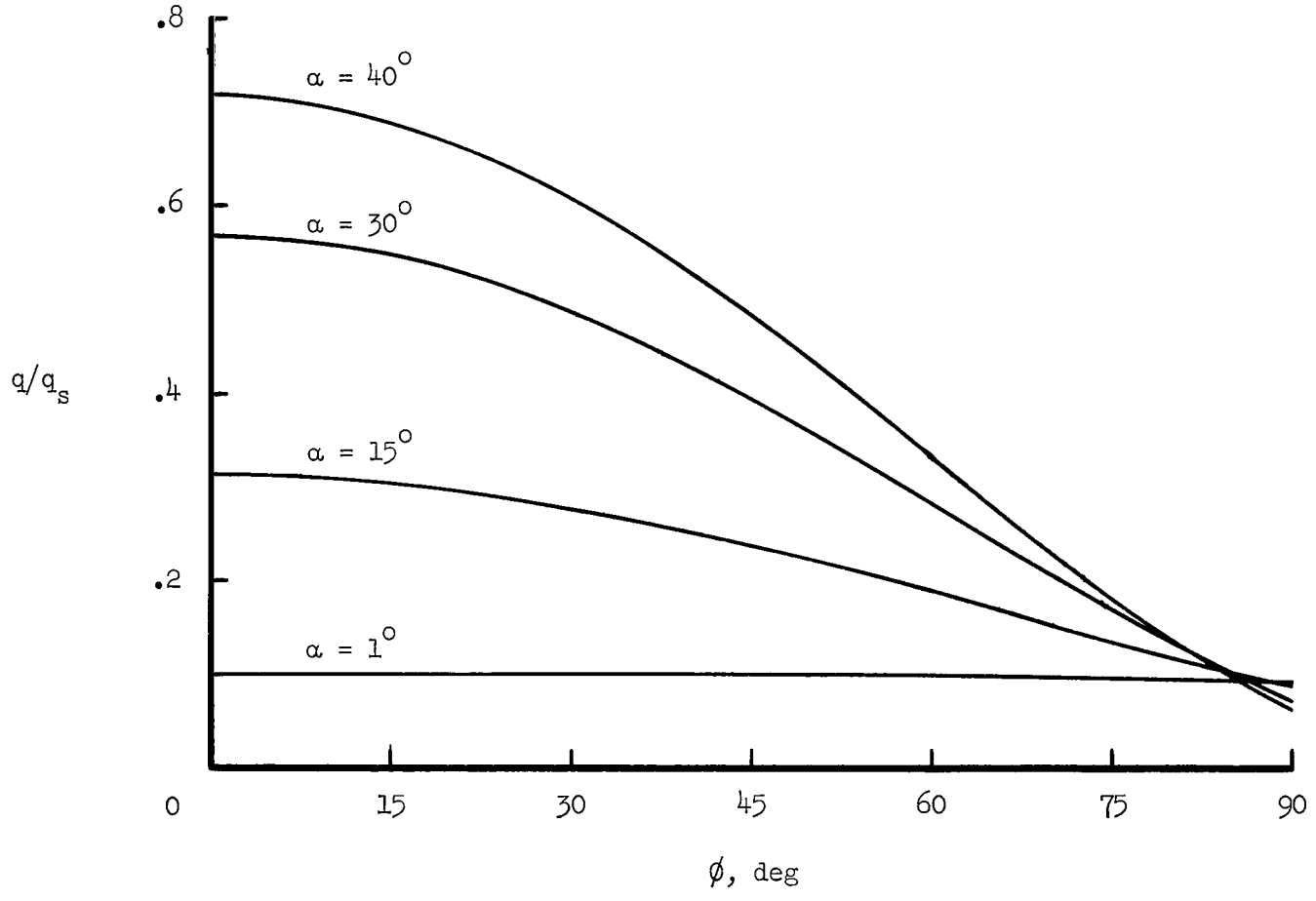

(a) s/r = 1.34 (tangent point).

Figure 16.- Circumferential heating-rate distribution for 13° blunted half-cone.

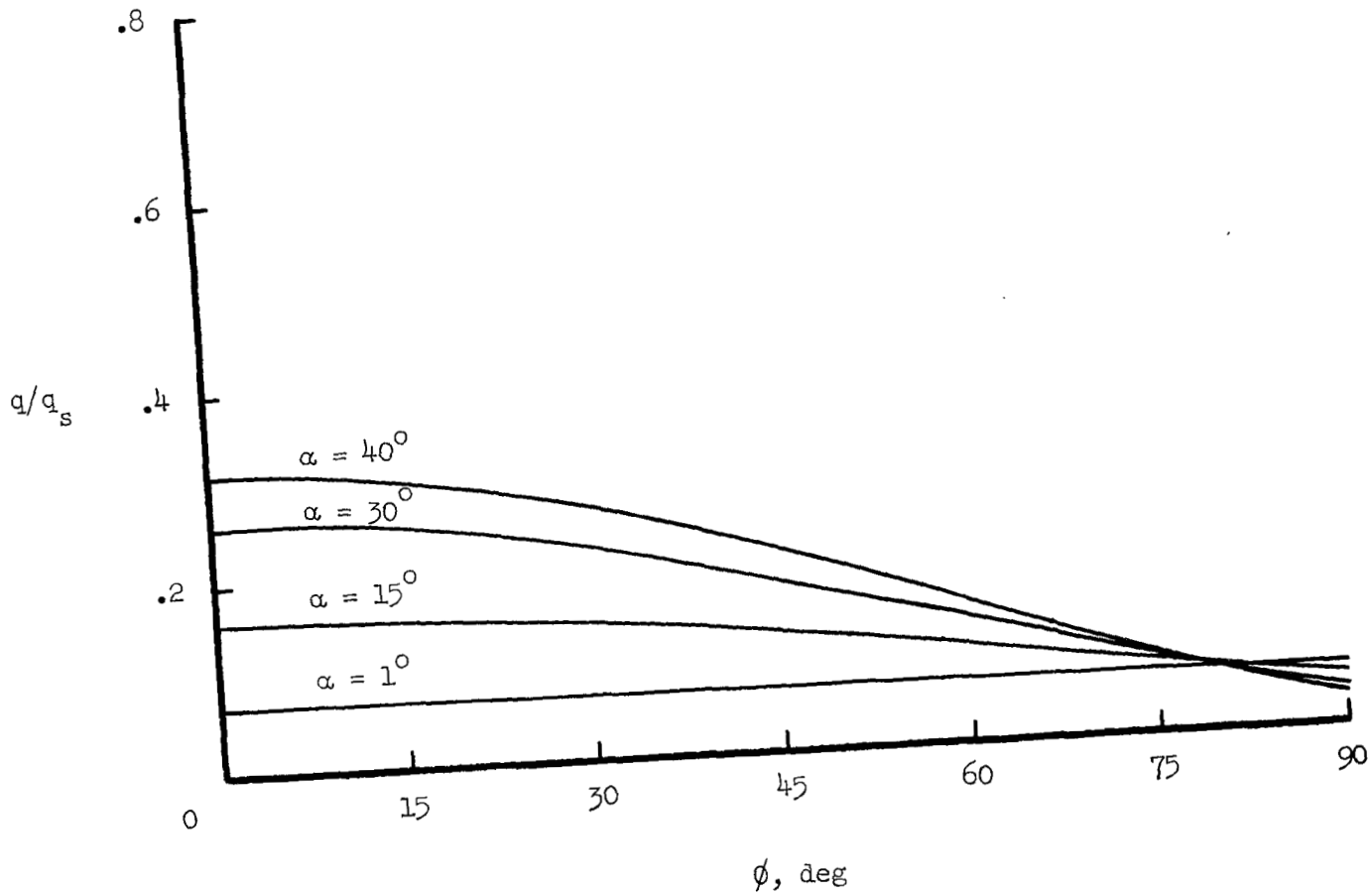

(b) s/r = 10.

Figure 16.- Concluded.

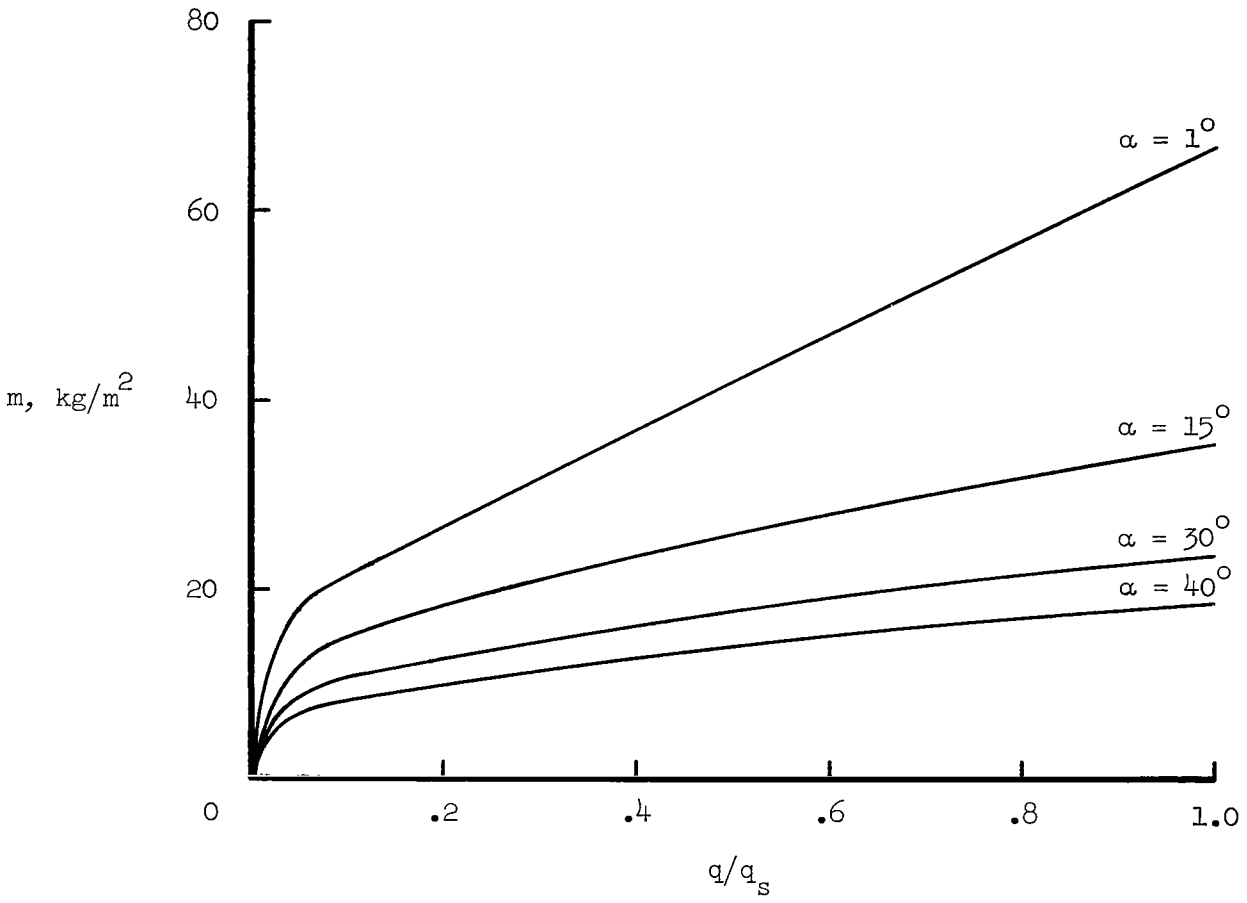

(a) 580 kg/m^3 phenolic-nylon.

Figure 17.- Effect of angle of attack on unit mass of ablation material required to limit back-surface temperature rise to 167^o K.

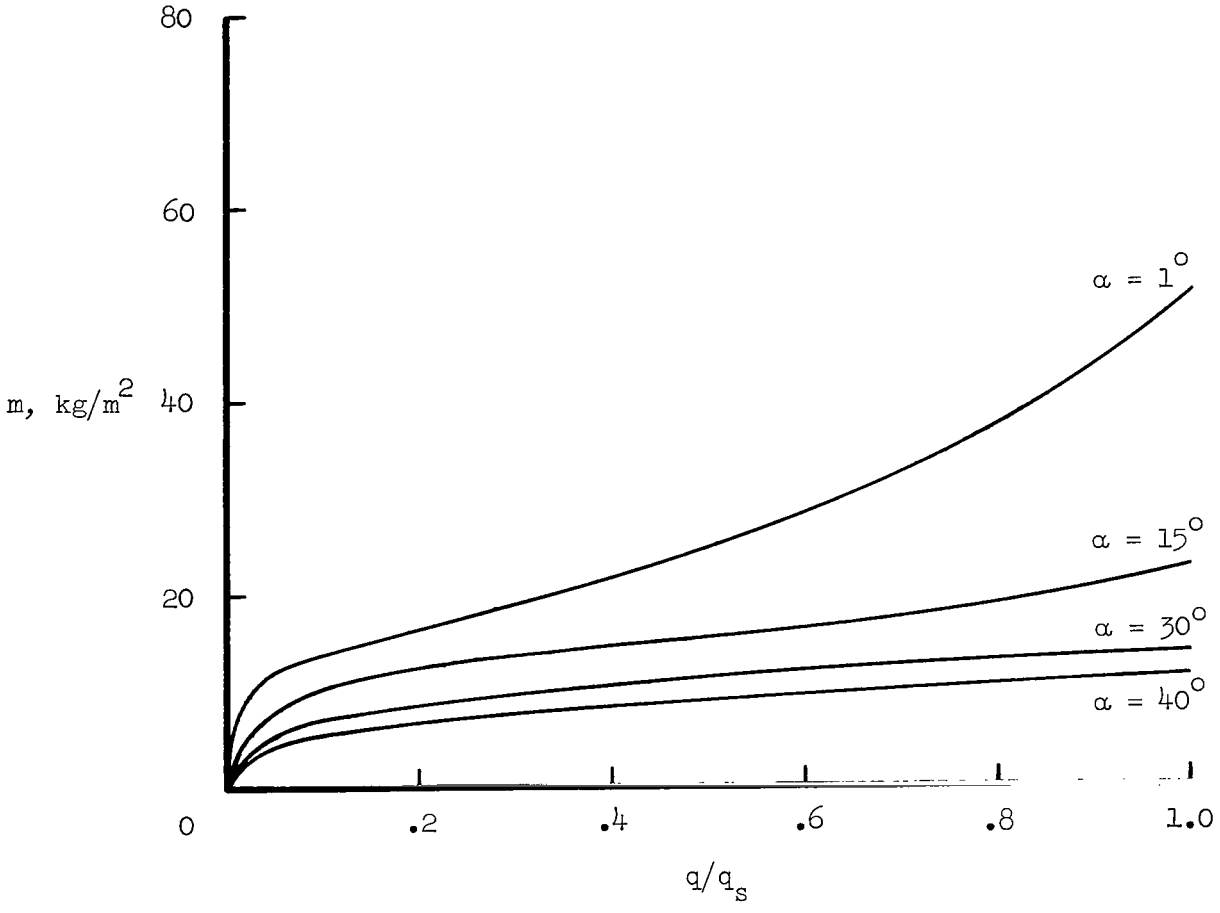

(b) 220 kg/m^3 phenolic-nylon.

Figure 17.- Concluded.

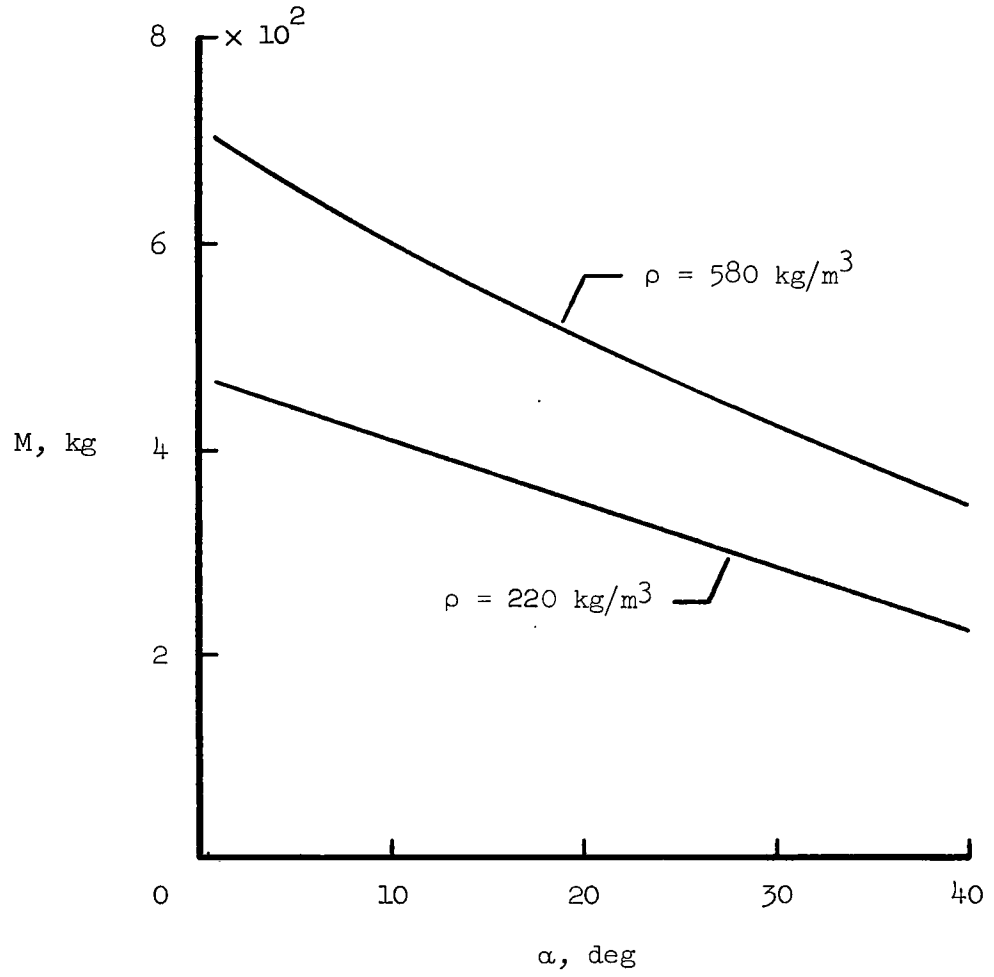

Figure 18.- Effect of angle of attack on the total ablative mass required for the windward surface of a 13^0 blunted half-cone for a 220 and a 580 kg/m^3 phenolic-nylon ablator.

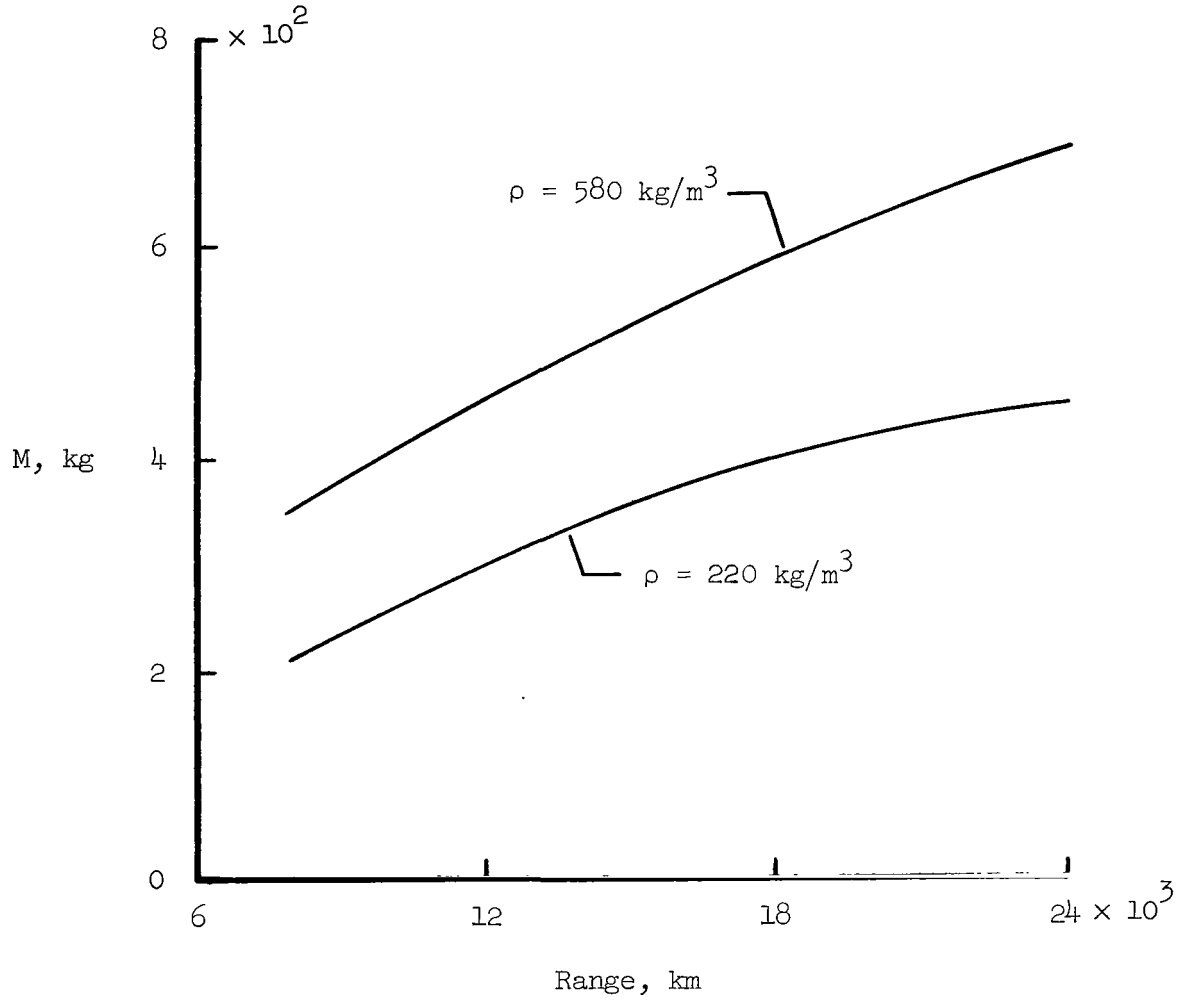

Figure 19.- Effect of maximum longitudinal range on the total ablative mass required for the windward surface of a 13° blunted half-cone for a 220 and a 580 kg/m^3 phenolic-nylon ablator.

NATIONAL AERONAUTICS AND SPACE ADMINISTRATION
WASHINGTON, D. C. 20546

OFFICIAL BUSINESS

FIRST CLASS MAIL

POSTAGE AND FEES PAID
NATIONAL AERONAUTICS AND
SPACE ADMINISTRATION

POSTMASTER: If Undeliverable (Section 158 Postal Manual) Do Not Return

"The aeronautical and space activities of the United States shall be conducted so as to contribute . . . to the expansion of human knowledge of phenomena in the atmosphere and space. The Administration shall provide for the widest practicable and appropriate dissemination of information concerning its activities and the results thereof."

—NATIONAL AERONAUTICS AND SPACE ACT OF 1958

NASA SCIENTIFIC AND TECHNICAL PUBLICATIONS

TECHNICAL REPORTS: Scientific and technical information considered important, complete, and a lasting contribution to existing knowledge.

TECHNICAL NOTES: Information less broad in scope but nevertheless of importance as a contribution to existing knowledge.

TECHNICAL MEMORANDUMS: Information receiving limited distribution because of preliminary data, security classification, or other reasons.

CONTRACTOR REPORTS: Scientific and technical information generated under a NASA contract or grant and considered an important contribution to existing knowledge.

TECHNICAL TRANSLATIONS: Information published in a foreign language considered to merit NASA distribution in English.

SPECIAL PUBLICATIONS: Information derived from or of value to NASA activities. Publications include conference proceedings, monographs, data compilations, handbooks, sourcebooks, and special bibliographies.

TECHNOLOGY UTILIZATION PUBLICATIONS: Information on technology used by NASA that may be of particular interest in commercial and other non-aerospace applications. Publications include Tech Briefs, Technology Utilization Reports and Notes, and Technology Surveys.

Details on the availability of these publications may be obtained from:

SCIENTIFIC AND TECHNICAL INFORMATION DIVISION

NATIONAL AERONAUTICS AND SPACE ADMINISTRATION

Washington, D.C. 20546